

Demography and life histories across the Roman frontier in Germany 400–700 CE

<https://doi.org/10.1038/s41586-026-10437-3>

Received: 28 February 2025

Accepted: 23 March 2026

Published online: 29 April 2026

Open access

 Check for updates

Jens Blöcher^{1,29}, Leonardo Vallini^{1,29}, Maren Velte², Raphael Eckel^{3,4}, Léa Guyon^{5,6}, Laura Winkelbach¹, Mark G. Thomas⁷, Nadia Gharehbaghi¹, Cassandra T. Mitchell¹, Jonas Schümann¹, Sophie Köhler¹, Elsa Seyr², Katharina Krichel¹, Sophie Rau¹, Jana Hirsch¹, Jana Duras¹, Paul Cloarec-Pioffet^{3,4}, Andreas Füglistaler^{3,4}, Kristin Klement¹, Miriam Wilkenhöner¹, Lisa Vetterditz¹, Francesca Gentilin¹, Melany Müller¹, Anna-Lena Mücke¹, Nicoletta Zedda⁸, Youssef Tawfik¹, Eveline Saal⁹, George McGlynn², Barbara Bramanti⁸, Jörg Orschiedt¹⁰, Regina Molitor¹¹, Barbara Fliß¹², Ines Spazier¹³, David Shankland¹⁴, Claus Vetterling¹⁵, Kurt Karpf¹⁶, Vera Planert¹⁷, Stefan Hölzl¹⁸, Silvia Codreanu-Windauer¹⁹, Dieter Quast¹¹, Ilija Mikic²⁰, Sven Fiedler²¹, Bernd Paffgen²², Maxime Brami^{1,23}, Thomas Richter²⁴, Raphaëlle Chaix⁶, Susanne Brather-Walter¹⁷, Peter Steffens²⁵, Markus Marquart²⁶, Thomas Becker²⁵, Jochen Haberstroh¹⁹, Mischa Meier²⁷, Sebastian Schmidt-Hofner²⁷, Sebastian Brather¹⁷, Michaela Harbeck², Steffen Patzold²⁸, Daniel Wegmann^{3,4} & Joachim Burger¹

The emergence of new political and social structures in Western and Central Europe during the transition from Antiquity to the Middle Ages has long been attributed to large-scale migrations. Yet emerging evidence increasingly emphasizes the role of small-group mobility in reshaping the Roman world^{1–3}. Here we present 258 ancient genomes from the former Roman frontier of southern Germany, which we analyse alongside 2,500 ancient and 379 modern genomes. Population genetic analyses reveal a major demographic shift coinciding with the late fifth century collapse of Roman state structures, when a founding population of northern European ancestry mixed with genetically diverse Roman provincial groups. Pedigree reconstruction and filia, a method for inferring the ancestry of unsampled relatives, indicate widespread intermarriage and minimal cultural differentiation. Genetic structure persisted through the sixth century, with admixture forming a population resembling modern Central Europeans by the early seventh century. Using Chronograph to refine the chronology of genealogically linked individuals, we estimate a generation time of 28 years, life expectancies of 39.8 years for women and 43.3 years for men, high infant mortality, and a society in which nearly one quarter of children lost at least one parent by age 10, yet most still grew up with grandparents. Pedigrees further reveal a society centred on nuclear families that practiced lifelong monogamy, strict incest avoidance, flexible lineage continuation and no levirate unions, indicating continuity with Late Roman social practices that later shaped the European family.

During the transition from Late Antiquity to the Early Middle Ages (fourth to seventh century CE), Central Europe experienced profound political, cultural and demographic changes, marked by the dissolution of Roman rule, the spread of Christianity, and new settlement patterns. The political landscape shifted dramatically, with the emergence of new polities in Western and Central Europe. Yet knowledge of local societies and the lives of non-elite people remains limited, as written sources are scarce and few settlements have been fully excavated⁴. Cemeteries linked to rural settlements therefore provide key information on this transition. From about 450 CE onwards, distinctive furnished ‘Row-Graves’ appeared across the former Roman frontier regions, from Northern France and the Netherlands to Northern Italy and Western Hungary⁵. These burials, often furnished with clothing,

weapons, jewellery or vessels, offer unique insights into everyday life and death in fifth to seventh century Europe⁶. The local societies associated with the Row-Graves in Southern Germany are usually characterized as small agrarian communities, sustained by crop cultivation and livestock (pigs and cattle), yet embedded in wider networks and developing social hierarchies. Some graves show Christian symbols by the end of the fifth century^{7–10}.

To broaden our understanding of demographic processes in this shifting socio-cultural landscape, we sequenced 221 Early Medieval genomes from multiple archaeological sites, with a focus on the northern frontier zone of the Roman Empire in present-day Southern Germany. We investigated Row-Graves from two regions: (1) the Danube-Isar area in Upper and Lower Bavaria, with a focus on Weilheim

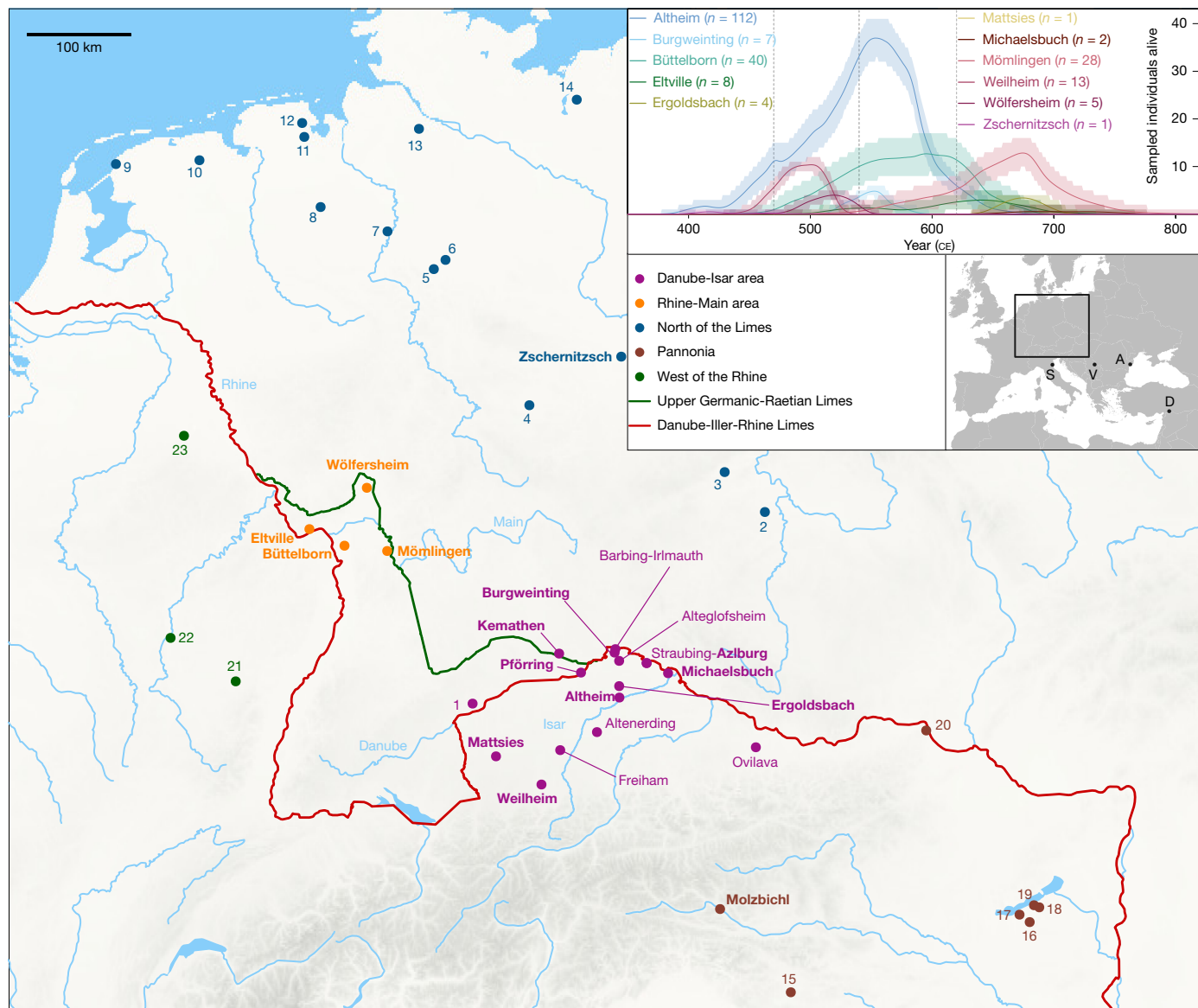


Fig. 1 | Location and chronology of the sites examined in this study. The Upper Germanic-Raetian Limes (green) marked the border of the Roman Empire until the second half of the third century CE, then replaced by the Danube-Isar-Rhine Limes (red) until the late fifth century CE. Late Antique sites (Azlbürg, Pförring and Kemathen) and Early Medieval sites with newly reported genomes are in bold characters, whereas sites from outside the core region are marked by letters: Viminacium (V), Argamum (A), Spina (S) and Doliche (D). Published reference sites are numbered: Niederstotzingen (1), Brandysek (2),

Konobrze (3), Hassleben (4), Hiddestorf (5), Anderten (6), Liebenau (7), Drantum (8), Midlum (9), Groningen (10), Zetel (11), Schortens (12), Issendorf (13), Häven (14), Ljubljana (15), Hács (16), Fonyód (17), Szólád (18), Balatonszemes (19), Klosterneuburg (20), Sarrebourg (21), Metz (22) and Alt-Inden (23). Top right inset, mean number (with 90% credible intervals indicated by shaded region) of sampled individuals alive at a given time according to Chronograph posterior estimates.

and Altheim—the latter notable for its securely dated early fifth century layers and extensive archaeological study¹¹; and (2) the Rhine-Main area, mainly represented by Büttelborn and Mömlingen (Fig. 1). During Antiquity, both regions were part of the Roman Empire. The Rhine-Main area belonged to the province of Germania Superior until the late third century CE, when the border was moved westwards to the river Rhine and the remaining provincial territory was reorganized as Germania Prima and Sequania until the dissolution of Roman rule during the fifth century. The Danube-Isar region belonged to Rhaetia Secunda until the collapse of the Western Roman Empire and probably came under Ostrogothic control in the late fifth century, though the extent of its reach remains debated¹². By around 540 CE, the region fell under Frankish influence, with a military command led by a duke (dux) that later evolved into the Duchy of Bavaria^{12,13}.

To assess the demographic and societal impact of these socio-political changes, we developed a novel Bayesian method, Chronograph, which jointly infers birth and death dates of all individuals by combining chronological signals from archaeological grave dating, radiocarbon measurements, genetic relationships and osteological age-at-death estimates (Supplementary Information 3). This approach yields precise birth date estimates: 50% of samples have 90% credible intervals narrower than 39.1 years, and 90% of samples have intervals smaller than 108.2 years. For individuals with identified close relatives, including those inferred from pedigree data, these intervals further reduce to 33.8 and 57.5 years, respectively (Extended Data Figs. 1 and 2, Supplementary Figs. 3.3–3.6 and Supplementary Table 2.3). In downstream analyses, we fully accounted for the remaining uncertainty using posterior samples of all individuals

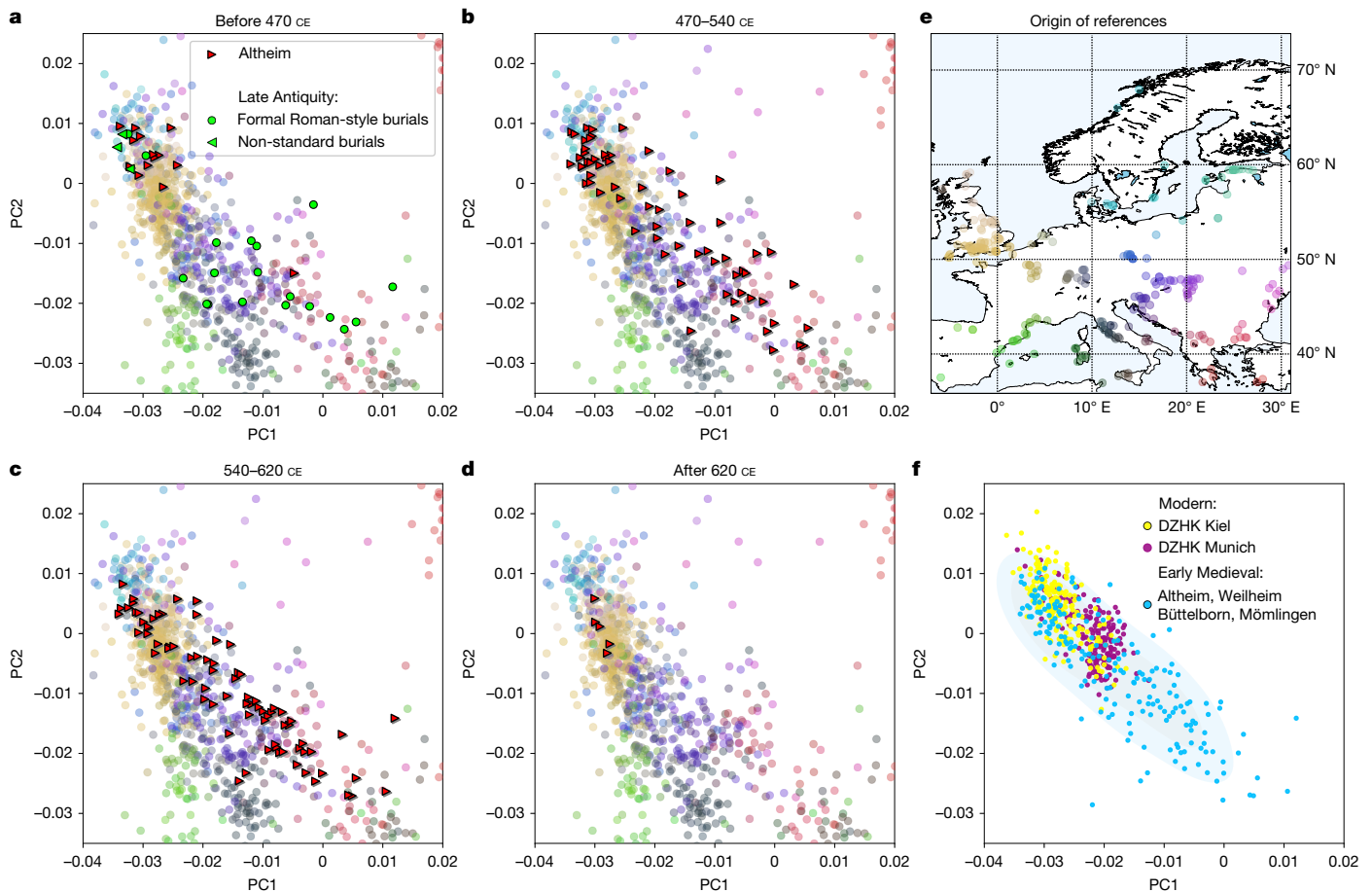


Fig. 2 | PCA of genetic variation in Altheim across time, alongside comparisons with Late Antique and modern populations. a–e. The chronology is based on individuals potentially alive during the time-window, estimated with Chronograph: before 470 CE (a), 470–540 CE (b), 540–620 CE (c) and after 620 CE (d). The background reference genomes represent genetic variation across Europe mainly from 800 BCE to 1 BCE, colour-coded by

geographic origin (depicted in e; for a larger version, see Supplementary Fig. 7.4). Genomes from Late Antiquity from the Danube-Isar region and Upper Austria shown in a are Azlburg and Ovilava (regular Roman-style burials); Pförring and Kemathen (non-standard burials). f, PCA of Early Medieval genomes with 75% contour lines compared to modern individuals sampled at two German hospitals: Munich (Southern Germany) and Kiel (Northern Germany).

alive at a given time or period (Fig. 1, top right, and Supplementary Fig. 3.7).

For comparative purposes, we supplemented the dataset with newly generated and published genomes from the fourth to eighth centuries in present-day Southern and Eastern Germany, Austria, Italy and Hungary^{14–21}. To explore genomic variability in earlier periods, we additionally sequenced 20 genomes from nearby Late Antique sites (Azlburg, Kemathen and Pförring) and 16 genomes from key sites across Europe and beyond (Viminacium, Serbia; Argamum, Danube Delta; Doliche, Anatolia; and Spina, Italy) (Fig. 1, Supplementary Information 1 and Supplementary Table 1), yielding a total of 258 newly generated genomes with a median depth of 2.25×. For Altheim, an additional 114 strontium isotope ratios were measured to further investigate patterns of individual mobility and migration (Supplementary Information 2).

Ancestry shifts and population structure

We first performed principal components analysis (PCA) to compare individuals from our main site, Altheim in the Danube-Isar region, with a dataset of more than 1,600 Iron Age and pre-Roman genomes from western Eurasia (Fig. 2c, Supplementary Tables 2 and 2.1 and Supplementary Fig. 7.4). This analysis revealed three distinct ancestry phases in the Altheim graveyard (400–470 CE, 470–620 CE and 620–660 CE), indicative of major demographic shifts (Fig. 2).

In the earliest phase (400–470 CE), fewer than 20 individuals (either directly sampled or implied by connecting sampled relatives up to third degree) were alive at any given time (Fig. 1, top right, and Supplementary Fig. 3.7). These individuals cluster with Iron Age northern Europeans (Fig. 2a, Extended Data Fig. 3 and Supplementary Figs. 7.3 and 7.4) and with present-day populations, above all from Northern Germany (Fig. 2), the Netherlands and Denmark (Supplementary Figs. 7.1 and 7.2), consistent with northern ancestral origins²². Hereafter, we use the term ‘northern ancestry’ to denote this genetic background. In the subsequent phase (470–620 CE), the number of identified individuals increased rapidly, reaching a peak of 70 around 550 CE (among whom 37 were sampled). Individuals from this period display a markedly broader distribution in PCA space than those from either the preceding or the following phases. Whereas some still overlap with Iron Age populations from Northern Europe, others show affinities to groups from the western Mediterranean or Southeast Europe, or fall entirely outside European genomic variation (Supplementary Figs. 1.2, 7.2 and 7.3), indicating a substantial influx of people with diverse ancestries. The PCA also shows that the Frankish takeover around 540 CE caused no detectable shifts in population structure (Fig. 2b,c).

The high inter-individual diversity observed in PCA space between 470 and 620 CE is mirrored in uniparental loci and in comparisons with present-day Germans from northern and southern cities (Kiel and Munich; Fig. 2f), highlighting the genetic heterogeneity of the population. However, overall autosomal genetic diversity estimates

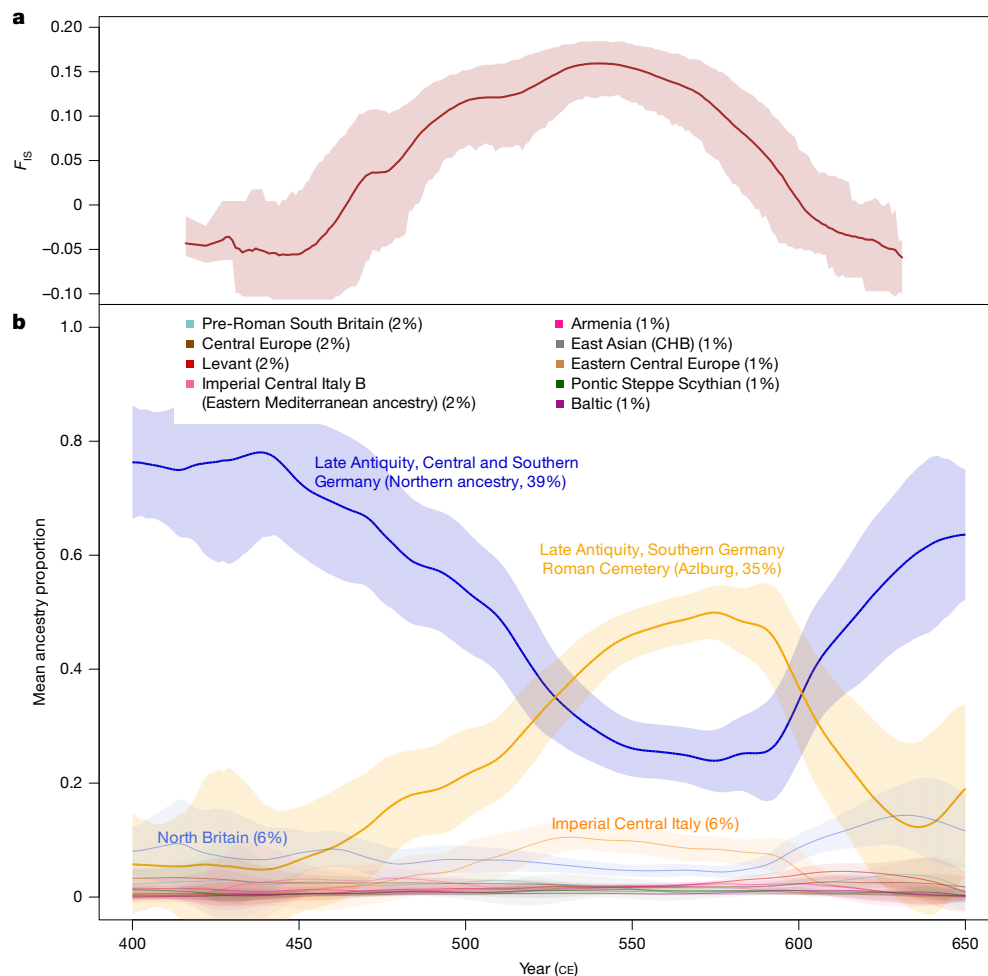


Fig. 3 | Temporal dynamics of substructure and ancestry in Altheim.

a, Deviation from Hardy–Weinberg equilibrium over time in Altheim measured as mean F_{IS} (solid line) for unrelated individuals sampled from 15,000 iterations. For a fine-scaled characterization of the shaded area. **b**, Mean ancestry

proportions of individuals alive at a given time in a model with 13 source populations, including local reference groups from the region; 95% credible intervals are indicated by the shaded areas.

(θ) are slightly higher in present-day populations (Extended Data Table 1). Although θ may be underestimated in historic genomes, this pattern suggests that Altheim during this period was more genetically structured, with individuals being less admixed. To examine this further, we quantified deviations from Hardy–Weinberg equilibrium (F_{IS}), and found that it increased sharply after about 470 CE, peaked around 550 CE, and then gradually declined towards the seventh century CE, consistent with transient substructure and a process of social integration (Fig. 3a and Extended Data Table 1).

For a fine-scaled characterization of the ancestral components contributing to the high genetic diversity at Altheim, we used the genealogy-based ancestry painting approach in twigstats²², based on ancestral recombination graphs from Relate²³, leveraging the resolution of whole-genome sequencing data (Fig. 3b, Supplementary Information 8 and Supplementary Tables 2.4–2.6). At a continental scale, the 470–620 CE population at Altheim can be modelled by source populations spanning Northern, Southern and Southeastern Europe (Supplementary Figs. 8.2–8.5), a pattern also supported by ancestry inference with ChromoPainter2 (ref. 24) and PANE²⁵ (Supplementary Information 8 and Supplementary Tables 2.7–2.10). More than three quarters of the ancestries identified can be attributed to co-occurring northern sources (Northern Europe (34%), North Britain (9%), Pearson's $r = 0.48$, $P < 0.001$; Supplementary Fig. 8.3) and southern or southeastern European sources (Roman Southeastern Europe (20%), Iron Age Central Italy (16%), $r = 0.21$, $P < 0.01$; Supplementary Fig. 8.3). Roman Southeastern

Europe stands out as a principal source population, a pattern further supported by Y-chromosomal haplogroup frequencies (Supplementary Information 6 and Supplementary Fig. 6.2), probably reflecting the role of the Balkans as a major recruitment hub for the Roman army²⁶. Contributions from Central Europe, Pontic Steppe and Baltic source populations remain minor.

Notably, however, the major ancestry sources, Northern Europe, Roman Southeastern Europe and Iron Age Central Italy were already represented in local groups within the study region before the emergence of the earliest Row-Grave cemeteries in Southern Germany (Fig. 2a). Prior palaeogenetic studies have suggested southward movements of northern European groups into Central Europe and Pannonia by the late fifth century^{15,19,22,27}, but the precise timing remained uncertain. Several newly sequenced individuals presented here, with northern ancestry, including those from Pfürring and Kemathen, as well as the earliest Altheim burials, Alh_61 (400–425 CE) and Alh_98 (412–414 CE), predate the Row-Grave horizon. Sharing patterns of chromosomal identical-by-descent (IBD) segments further corroborate evidence for an earlier migration from the North into the Roman frontier zone: long IBD segments (>20–400 cM) connect sites within the Danube-Isar area, whereas only shorter segments (<20 cM) are shared between individuals from Danube-Isar and Rhine-Main sites, consistent with a degree of regional isolation (Extended Data Fig. 4 and Supplementary Fig. 10.1). Together, these findings indicate that many individuals with northern ancestry were

already established in the Roman frontier zone by the late fourth century.

Roman Southeastern European ancestry was likewise established in the region by the fourth century CE. At the nearby Roman military base of Azlburg, most individuals carried this component alongside Iron Age Central Italian ancestry, while others also exhibited northern European sources, reflecting the diverse composition of the Late Antique Roman military. The population of Altheim can be modelled well using these local sources (Fig. 3b).

Strontium isotope data are consistent with a predominantly local origin of most Altheim individuals. Only a minority of Altheim individuals show non-local signatures, that could theoretically derive from several regions outside of the Bavarian Alpine foothills but in light of the archaeological and historical context, are more likely to originate from less distant areas north of the Danube. Notably, the earliest six identified non-locals were all women. The proportion of non-locals declines from about 35% (90% credible interval: 21–50%) around 470 CE to about 7% (90% credible interval: 3–12%) by 540 CE, and disappears entirely by 620 CE (Extended Data Fig. 5 and Supplementary Fig. 2.2), indicating reduced mobility during the phase of increased population structure and subsequent admixture, and in line with trends in the wider region²⁸.

The emerging scenario depicts a population of northern ancestry, already established in the frontier zone and potentially supplemented by continued influx from the North, incorporating substantial Azlburg-like ancestry from neighbouring Roman contexts from 470 CE onwards. Concurrently, burial activity at Altheim shifted to the north-eastern section of the cemetery (Extended Data Fig. 6, Supplementary Fig. 14.1 and Supplementary Video 1). Over the following 150 years, interactions between the founding groups with northern ancestry and later arrivals from Roman provincial communities produced high genetic diversity and population substructure. As admixture proceeded on site (direct evidence presented below), both inter-individual diversity and substructure gradually declined. Individuals buried after 620 CE again cluster with modern and Iron Age northern and central European genomes, but compared with the first phase they are shifted slightly towards southern and southeastern European individuals in PCA space. During this period, the number of sampled individuals drops to around 10, either reflecting a true demographic contraction or more likely a shift in burial practices to as-yet unsampled or unexcavated areas¹¹. However, the presence of several close relatives among these samples may exaggerate the apparent speed at which genetic ancestry converges during this period towards what later forms the characteristic genetic signature of southern Germany (Fig. 2f).

Similar demography across South Germany

Data from other Early Medieval cemeteries in Southern Germany (Fig. 1) align with the model established for Altheim, indicating comparable demographic processes across regions. Although smaller sample sizes limit chronological resolution, sixth century sites consistently show wide ancestry variation, ranging from Northern to South or Southeastern Europe (PCAs in Supplementary Information 1 and Supplementary Fig. 7.2). This applies also to inland sites deep within long-settled former Roman territory and far from the frontier, such as Weilheim (480–540 CE), whose ancestry, as for post-470 CE Altheim, can be modelled by these proxy sources: 37% from the Roman cemetery of Azlburg, 34% northern ancestry sampled in Central Europe, and 12% from Northern Britain (Supplementary Fig. 8.8). If a proportion of northern ancestry plausibly derived from distinctly Roman military or related civilian contexts, then the majority of ancestry in the late fifth to early sixth century Row-Grave cemetery would have been genuinely Roman in origin. In the Rhine-Main region, sixth century genomes from Eltville, near Moguntiacum (modern Mainz), similarly resemble Altheim's middle phase (470–620 CE). A comparable composition is

observed two to three generations later at Büttelborn and Mömlingen (Supplementary Fig. 9.1).

Alongside broadly similar patterns, comparison of the Rhine-Main and Danube-Isar regions reveals a few notable differences. The Danube-Isar Early Medieval genomes carry higher Iron Age Central Italy ancestry, whereas those from the Rhine-Main region show higher British (both Northern Britain and Pre-Roman south Britain), Eastern Central Europe and Baltic ancestry (one-sided Mann–Whitney U test, $P < 0.05$, Supplementary Fig. 8.4). This pattern corresponds to the variation observed in PCA space: the Rhine-Main cluster lacks the southernmost component of the gradient, indicating partly distinct ancestral sources rather than simply changing proportions of the same ones. Consistent with these differences, F_{ST} values between settlements are high and clearly exceed those observed between modern northern or southern German populations (Extended Data Table 1).

Although an overall blending of ancestries is evident throughout, reflective of broad supra-regional demographic shifts, distinct individual ancestries persist well into the later phases of the Row-Grave horizon. At Altheim, six individuals dating to the sixth century show ancestries predominantly attributed to Italian sources, with only minimal northern admixture. At Michaelsbuch, two individuals still, even in the eighth century, carry ancestries that are strikingly atypical for the region today, reflecting lingering pockets of post-Roman structure, later gene flow from outside the area, or a mixture of both. More distant ancestries are also apparent: a male from Altheim (Alh_245; 528–553 CE) who shares long IBD segments with individuals from the Berel necropolis in modern Kazakhstan, derives roughly two-thirds of his ancestry from East Asian sources and one-third from populations of the western Steppe. A contemporary male from Wölfersheim (W67) carries similar, albeit less of this Asian ancestry, whereas late fifth century females with artificial cranial deformation (Wh4 and Wh59) lack Steppe-related ancestry and instead exhibit patterns consistent with post-Roman admixture¹⁴.

From a historical perspective, individuals from Altheim predating 470 CE may have been descendants of Roman soldiers or peasants who had lived in the frontier zone, or they may have been settled in the Altheim area as agrarian workers by Roman authorities in the early fifth century². As Roman authority waned in the later fifth century, the collapse of military and economic structures loosened the social and legal bonds that had tied dependent peasants, such as *coloni* and slaves, to their landlords, thereby facilitating regional mobility. Although long-distance migration cannot be ruled out in individual cases, it is not necessary to explain the emerging genetic patterns. Instead, the regional mobility of day labourers, merchants, and others likely sustained a steady influx into Altheim during the sixth century. Furthermore, military conflicts in the Danube-Isar region may have displaced local peasants and mobilized armed groups. A similar scenario may explain the genomic patterns observed in sixth century individuals in the Rhine-Main region: with the dissolution of Roman military structures along the Rhine frontier in the fifth century and the accompanying collapse of economic and social networks, individuals, families and groups began to move, some of them across the river Rhine, establishing new communities or joining existing ones.

Demographic shift linked to intermarriage

To evaluate the consequences of the inferred demographic shifts at the family level, we reconstructed pedigrees and applied *filia*, a novel method that leverages familial relationships to infer f_4 -statistics for unsampled individuals (Supplementary Information 13 and Supplementary Table 2.11). At Altheim, this approach reveals immediate intermarriage between individuals of predominantly northern European ancestry and those with Roman Azlburg-like ancestry, indicating rapid integration of newcomers, regardless of their individual ancestry, into the local community (Fig. 4). Analysis of the 24 individuals with the

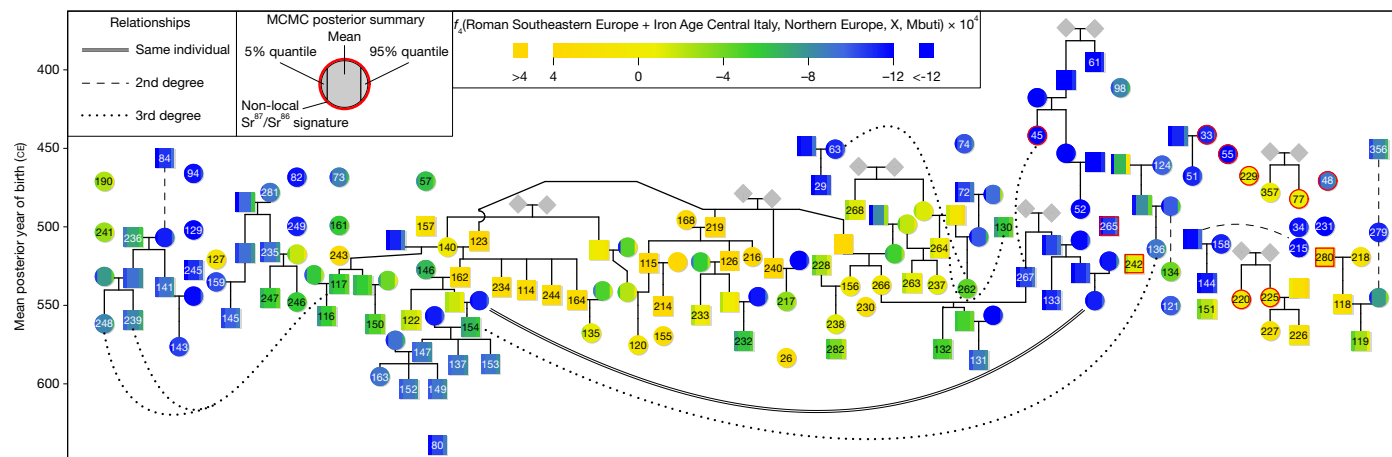


Fig. 4 | Reconstructed pedigrees of Altheim with colour-coded f_4 -statistics presented in a chronological context. Sampled individuals are numbered and inferred individuals are depicted by empty markers. Individuals not

connected to a pedigree are displayed for contextual reference. All f_4 -statistics were inferred with filia. Red outlines indicate individuals of non-local origin based on strontium isotope analysis. MCMC, Markov chain Monte Carlo.

most extreme f_4 values shows considerable individual and chronological variation in grave furnishings, but no systematic differences between burials of individuals at the high versus low ends of the distribution (Supplementary Table 2.12). Although the archaeological interpretation is somewhat complicated by the apparent reopening of many burials¹¹, this pattern suggests that material culture was largely decoupled from genetic ancestry. These findings contrast with those from Szólád in Pannonia and Collegno in Northern Italy^{15,29}, as well as with Burgweinting near Altheim, where two adjacent burial groups differ sharply in ancestry and material culture: four women of nearly exclusive northern ancestry were buried with lavish goods, whereas a neighbouring mixed-ancestry group had modest furnishings (Supplementary Fig. 1.9). By contrast, Altheim reflects a simpler rural lifestyle, without comparable social or cultural differentiation.

Life-history parameters

Fine-grained demographic data on local societies in Late Antique and Early Medieval Europe remain scarce. For the Roman Empire, epigraphic and literary sources provide diverging estimates of mortality and marriage ages^{30,31}. In Early Medieval Provence, a study of more than 1,000 peasants indicates that boys and girls became eligible for marriage at around the age of 12, life expectancy at birth was about 20 years, and women married earlier than men while generally avoiding remarriage³². At Altheim, using birth and death dates inferred by Chronograph, we could generate reliable estimates of key life-history parameters for a local Early Medieval community. Both infant and child mortality were higher for boys than for girls, with 9.7% (90% credible interval: 9.7–9.7%) and 7.8% (90% credible interval: 7.7–8.3%) of all identified boys and girls, respectively, not reaching the age of seven (Supplementary Fig. 3.8). Nonetheless, men had a higher life expectancy (43.3 years, 90% credible interval: 41.6–45.2) than women (39.8, 90% credible interval: 38.5–41.1), driven by a higher mortality of females after about 10 years of age (Fig. 5 and Supplementary Fig. 3.8), suggesting that giving birth was a major risk factor. The mean generation time was 28.0 years (90% credible interval: 26.4–29.6; Fig. 5 and Supplementary Fig. 3.9). Half-orphans were relatively common, with 11.3% (90% credible interval: 6.4–17.0%) and 25.5% (90% credible interval: 17.7–34.0%) of all children having lost at least one parent by the age of five and ten, respectively, whereas only 0.5% (90% credible interval: 0.0–1.9%) and 2.5% (90% credible interval: 0.0–5.9%) had lost both parents by the same age, respectively (Supplementary Fig. 3.11). However, the majority of children grew up with grandparents: 81.8% (90% credible interval: 54.6–100%) of all children had at

least one grandparent alive at birth and 67.4% (90% credible interval: 30.0–90.0%) had at least one grandparent alive at ten years of age (Supplementary Fig. 3.11). Although we estimate that mothers were on average 0.7 (90% credible interval: –6.5–11.7) years younger than their partner, posterior support for an older father exceeded 90% for only 5 out of 77 couples (6.5%; Supplementary Fig. 3.10).

Family structure and cultural legacy

There is a long history of research examining family structures between Late Antiquity and the Early Middle Ages, as well as the influence of Christianity, as key factors in the development of modern European kinship systems^{30,33–36}. However, sources are mostly normative texts or document elite practices, whereas little is known about non-elite local societies beyond the findings of a small number of genomic studies, all from geographically, chronologically or culturally distinct regions^{37–41}. To evaluate spatial clustering among kin, we analysed grave distribution at Altheim (Supplementary Fig. 14.1) and Büttelborn (Fig. 6). At Altheim, first- to fourth-degree relatives ($N = 77–137$) were buried significantly closer together than unrelated individuals ($n = 3,007$; Mann–Whitney U test, two-sided, $P < 1.08 \times 10^{-17}$ to 1.04×10^{-3}), with spouses ($n = 6$) also interred in close proximity (Supplementary Information 14). At Büttelborn, spatial placement was also shaped mainly by close biological relatedness, with distant kin exerting little influence. For example, a father, mother and three children occupy a circular cluster separated from more-distant relatives, such as an aunt and distant cousins (Fig. 6). Assuming that burial proximity reflects social relations, these patterns are consistent with communities being organized around nuclear or stem families, sometimes complemented by extended kin, such as half-siblings. This is reflective of global patterns in agrarian societies, in which small core family units are typically embedded within broader kin networks⁴², and aligns with historical research on local societies since the early Roman Empire³⁵ and in Southern Germany after about 750 CE (ref. (43)).

Drawing on reconstructed pedigrees from Altheim (Fig. 4) and Büttelborn (Fig. 6, Extended Data Fig. 7 and Supplementary Fig. 12.2), we examined which rules of residence and descent are compatible with such data. Pedigrees more often continued through sons (20 and 9 cases in Altheim and Büttelborn, respectively; Supplementary Table 14.3), although continuation through daughters also occurred (9 and 2 cases, respectively; Supplementary Table 14.3). At Büttelborn, five generations of male relatives (Fig. 6, red pedigree), were buried in a tight cluster. By contrast, much less spatial clustering can be observed for the individuals of a pedigree connecting mostly

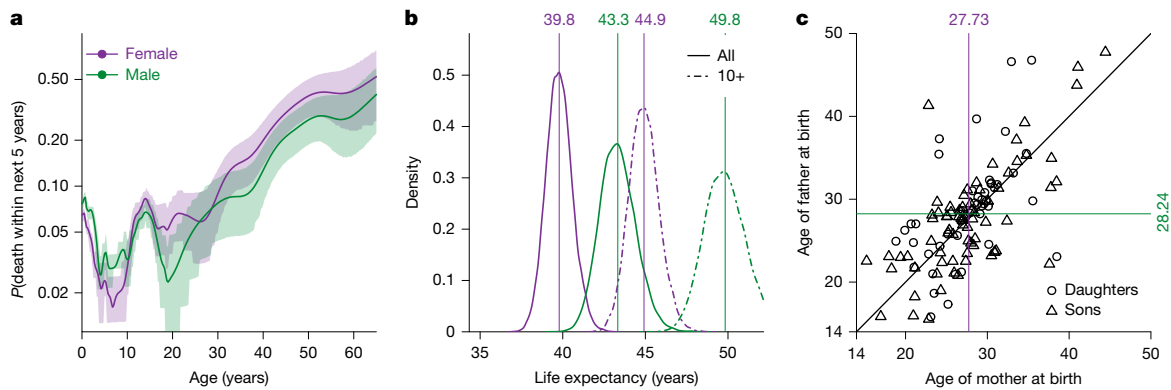


Fig. 5 | Life history traits inferred by Chronograph. **a**, Posterior mean (solid line) and 90% credible interval (shaded region) of the fraction of individuals alive at a given age that die within the next five years. **b**, Posterior distribution (curve) and mean (vertical lines) life expectancy (average lifespan) for all individuals (solid curves) or those that survived at least until 10 years of age

women over four generations (Fig. 6, orange). Across sites, women share significantly larger IBD segments with individuals buried elsewhere than men (Mann–Whitney U test: two-sided, $P < 0.0442$; Supplementary Table 10.3 and Supplementary Figs. 10.8–10.11). Within sites, however, they share far fewer IBD segments (>8 cM) in comparison to men (Altheim: 30.92 ± 5.28 versus 170.55 ± 13.08 ; Mann–Whitney U test: two-sided, $P < 1.47 \times 10^{-61}$; Supplementary Table 10.2), and their relatedness coefficient is 6-fold lower at Altheim and 1.5-fold lower at Büttelborn. These inferred patterns are consistent with a flexible patrilocal system in which most women resided near their husband’s family, whereas some men settled near their wives (Supplementary Information 14), particularly in the absence of a son. However, the high Y-chromosomal and mitochondrial diversity at both sites is incompatible with strict patrilineal descent and strict patrilocality^{44,45}. Instead, it indicates a flexible patrilineal or a bilateral system with flexible patrilocality in which pedigrees were continued mainly through sons but occasionally also through daughters. We further observed that, at least in Altheim, unions were predominantly exogamous when the pedigree continued through sons (16 out of 21 cases), whereas endogamy was more common when continuity was through daughters (5 out of 9 cases), a pattern that echoes those documented in modern matrilocal or matrilineal societies⁴⁶. Together, patterns of residence and descent in Early Medieval Southern Germany closely mirrored those established during the Late Roman period. Written sources from the Roman Empire show a constant trend towards a bilateral inheritance system: in Roman law, daughters could, under certain circumstances, inherit equally with sons in cases of intestate succession. Yet restrictions on the ability of women to bequeath property, together with other succession rules, generally ensured that assets passed through the male line. From the early centuries CE onward, however, inheritance through daughters was gradually reinforced, a development that continued into Late Antiquity⁴⁷. Wills sometimes privileged male descendants who received a larger share, especially when land was concerned, but daughters were often treated equally and, in the absence of sons, even became primary beneficiaries (ref. 48, pages 62–71). In the fifth and sixth centuries, both Western Roman and Justinianic law, as well as legal practice in western post-Roman kingdoms, provided further security for the inheritance rights of daughters and their children by will or on intestacy, and thus strengthened bilateral succession (ref. 48, pages 71–72). At the same time, in Late Roman society, family tradition was increasingly conceived of as deriving from both paternal and maternal lines³⁵.

In the Late Roman and post-Roman West, Christian societies increasingly emphasized lifelong monogamy: while divorce faced stricter legal regulation, widowhood was elevated and remarriage was considered

with more than 90% posterior support (dot-dashed curves). **c**, Posterior estimates of the mean age of mother and father at birth for each identified child (multiple children per parent). Solid coloured lines indicate the resulting posterior mean estimate of the generation time for women (purple) and men (green).

morally problematic^{30,33,36,47}. Marriages between close kin were condemned, prompting numerous prohibitions by church councils and secular authorities from around 500 CE onward³⁴. Christianity thus reinforced earlier social trends: literary and epigraphic studies indicate that close-kin marriage was already largely avoided in the pre-Christian Roman West, and lifelong monogamy had become a widely promoted ideal^{30,34,49}. The *Lex Baiuvariorum* (tit. VII, 1), issued in the eighth century but reflecting earlier norms, confirms strict prohibitions of incest and levirate unions for Bavaria, where historical and archaeological research indicates the continued influence of Christianity after the collapse of Roman rule¹³. In line with these written sources, our data suggests that lifelong monogamy, with limited divorce or remarriage of widows, was the prevailing norm in sixth century Southern Germany: we identified 68 probable single-partner unions but only five individuals in Altheim and Büttelborn (three men and two women) who had children with multiple partners, and none of the cases is chronologically incompatible with serial monogamy (Supplementary Fig. 3.12). Although we cannot entirely rule out that children from other partnerships either did not exist or were buried elsewhere, the substantial coverage of our sample at Altheim (38%, 90% credible interval: 22–55%; Extended Data Table 1, Supplementary Information 12 and Supplementary Fig. 12.4) makes it unlikely that such a pattern would have systematically escaped detection.

The near absence of long (>12 cM) runs of homozygosity (Supplementary Table 2.13) and the lack of shared IBD segments (>8 cM) between spouses support strict incest avoidance, excluding relationships closer than the sixth degree (Supplementary Table 11.1). Given the small estimated community size (maximum of around 70 individuals per settlement per generation; Extended Data Table 1 and Supplementary Information 16), such avoidance probably encouraged intermarriage across broader social networks. However, a comparable absence of relatedness between spouses was also observed in endogamous unions, that is, among partners from Altheim. Recent genetic research suggests that incest avoidance was also present in non-Christian societies, such as Iron Age populations from the British Isles⁵⁰, and Avar societies in the Western Pannonian plains^{37,51}. However, the latter show evidence for levirate unions, which are absent in Altheim and Büttelborn, in accordance with the *Lex Baiuvariorum*.

Overall, Altheim is characterized by patrilocal tendencies and either patrilineal or bilateral descent rules, with pedigrees continuing through daughters more frequently than at previously studied sites (Supplementary Table 14.4), except in a matrilocal Iron Age society in southwest England⁵⁰. The rate of multiple reproductive unions is low (Supplementary Table 14.4), and only a Neolithic community in north-central France shows a lower rate⁵². These findings align with written sources

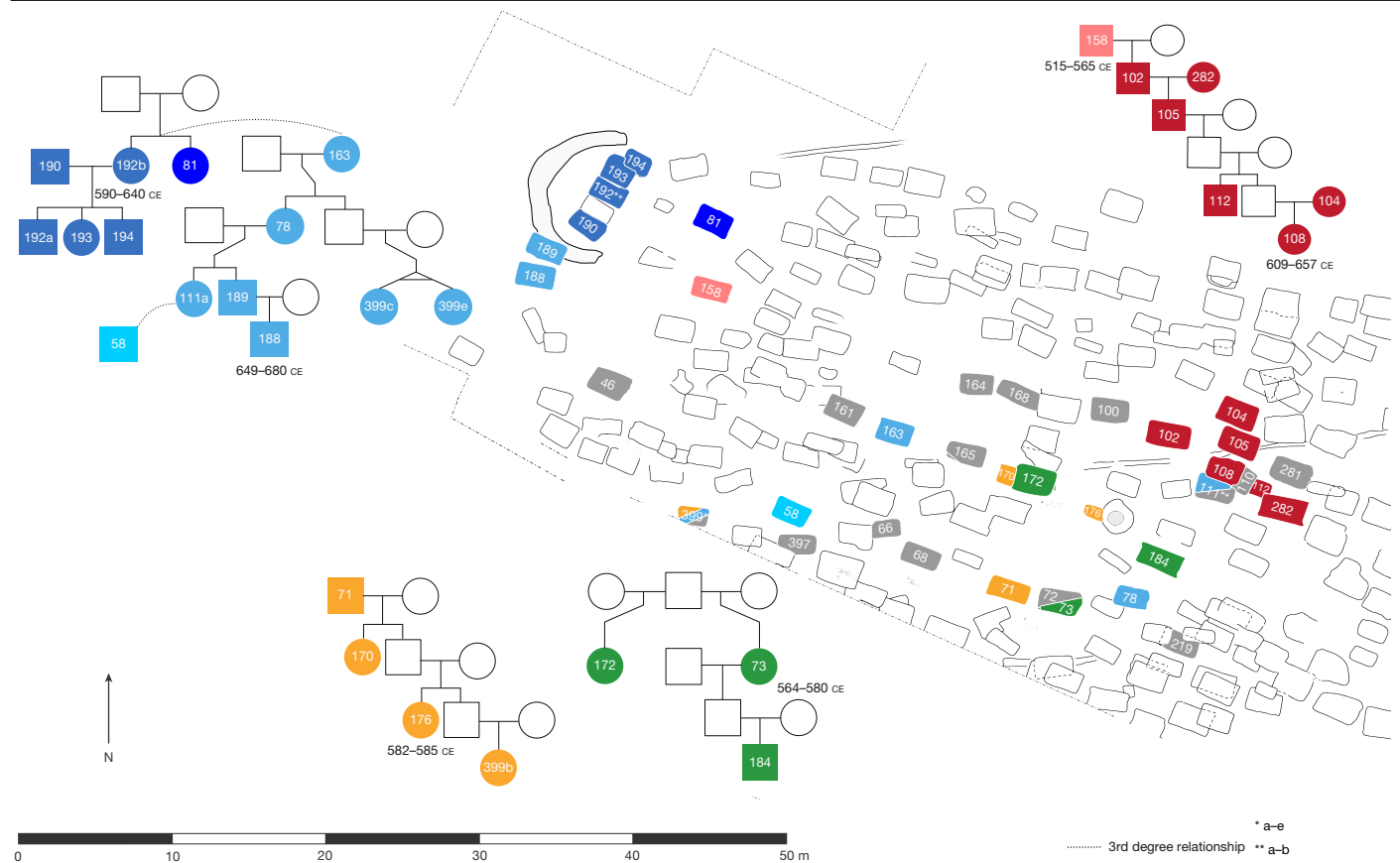


Fig. 6 | Spatial arrangement of reconstructed pedigrees in the Büttelborn cemetery. Colour-coded pedigrees mapped onto individual graves; graves of unrelated individuals are shown in grey. Chronograph estimates of birth and

death dates are shown for individuals with a ^{14}C date. A corresponding depiction for Altheim is provided in Supplementary Fig. 14.1. Grave plan courtesy of Thomas Becker, hessenARCHÄOLOGIE, Außenstelle Darmstadt.

and suggest that by the sixth century CE, Central European agrarian societies already maintained residence, and marriage practices that were to become characteristic of Latin Christian Europe.

Rethinking the transition

Although the transition from Late Antiquity to the Early Middle Ages has traditionally been framed as a conflict between northern ‘barbarians’ and a Roman Empire in decline, newer studies reveal a multifaceted transformation^{1,3,19,29,53–55}. The integration of genomic, isotopic, written and archaeological evidence now provides a clearer view of demographic, cultural, and social dynamics in Central Europe, particularly regarding the everyday life of agrarian societies. Although most of the demographic processes described here occurred locally, they developed within the framework of earlier north-to-south migrations towards the Roman frontier. Analysis of long IBD segments (>20 cM) among individuals confirms extensive transregional migrations well before the emergence of the Row-Grave cemeteries. Thirty-seven individuals from the Rhine-Main and Danube-Isar regions share long segments with contemporaries from sites more than 200 km apart, spanning Northern Germany, the Netherlands, England, Austria, Hungary, Croatia and as far as Viminacium in eastern Serbia (Extended Data Fig. 4, Supplementary Figs. 10.1–10.7 and Supplementary Information 10). IBD sharing is strongest among northern ancestry individuals and decreases along PC1 (Spearman’s $R = -0.89$, $P < 9.04 \times 10^{-8}$). Biological kinship data indicate that this migration involved individuals and small kin groups rather than entire populations, with likely second cousins buried more than 270 km apart (Büttelborn–Hiddestorf), and multiple links connecting the Danube-Isar region to elite burials at Szólád (around 500 km away) and cemeteries near Vienna (for more details on

transregional IBD networks, see Supplementary Information 10 and 12). Subsequent movements unfolded against this demographic landscape, largely established by the turn of the fourth to fifth century. Although it remains unclear whether these biological relationships correspond to social ties recognized by the individuals themselves, they may reflect transregional networks that fostered familial and social connections across Central Europe, extending to Pannonia and Northern Italy¹⁵. The persistence of such networks, embedded within Roman-influenced traditions and infrastructure, may have facilitated the later rapid and cohesive spread of the Row-Grave horizon across Early Medieval Europe.

At Altheim, burials first appeared around 414 CE, initially isolated in the landscape and belonging to individuals of northern European ancestry with genomic profiles distinct from those of central European Iron Age populations (Supplementary Fig. 7.9). Although migration from the north probably continued, the majority of these early individuals and those who followed probably descended from families long established within or near Roman territories. They may represent descendants of Roman soldiers who had lived in the frontier zone or peasants who were settled in the wider Altheim area as agrarian workers by Roman authorities in the early fifth century². Although their ethnic or social self-identification remains unclear⁵⁵, their predominantly intra-group marriages until the pivotal 470 CE horizon suggest a shared sense of belonging, possibly reinforced by legal restrictions on marriage applied to *coloni* and other non-elite groups⁵⁶. Their burials combined Roman-influenced and other practices forming a hybrid culture of inhumation and furnishing of graves with clothing and jewellery that foreshadowed features of the Row-Grave horizon¹³.

The demographic shift around 470 CE saw people with ancestry typical of Roman towns and forts begin to move into the hinterland,

being buried across Row-Grave cemeteries of Early Medieval Southern Germany. In line with findings for other regions of the Late Antique West², the collapse of Roman structures in the late fifth century had probably weakened ties binding peasants to their land in Southern Germany, enabling regional mobility and sustaining a steady influx into local communities throughout the sixth century. Although ancestries are not identical between sites, reflecting the distinct genetic composition of Roman settlements in each region, the general process of derivation from Roman provincial populations is broadly similar across Southern Germany. Although long-distance migration probably occurred in individual cases or small groups—for instance, links between Altheim and sites such as Mödling and Czocorgasse³⁷ probably reflect stepwise or direct movements into the Vienna Basin during the sixth century—large-scale migrations are not necessary to explain the broader emerging genetic patterns in Southern Germany after 470 CE.

Over the following 150 years, intermarriage produced a population already genetically resembling modern Central Europeans, including southern Germans, with individuals of northern ancestry contributing disproportionately due to their numerical dominance, probably maintained by ongoing mobility. Roman-related ancestry left a modest but enduring signal in our study region, subtly modified by later northern and eastern inputs^{41,57}, all of which remain detectable in genomes from present-day Germany (Extended Data Fig. 8 and Supplementary Fig. 8.22). Culturally, these local societies continued Roman practices of flexible inheritance and appear to have embraced Christian ideals such as lifelong monogamy, with minimal divorce or remarriage after widowhood. They also strictly avoided incest and levirate unions. Whether this pattern was unique to the Rhine-Danube frontier or part of broader trends across former northern frontier zones of the Roman empire remains to be investigated, but evidence from the Rhine-Main area presented here suggests wider applicability.

The genomic patterns in Southern Germany may also shed light on the region's medieval vernacular, the everyday language spoken by people^{15,19,22,27}. Networks among individuals of northern ancestry could have facilitated the spread of early Germanic dialects into Southern Germany, where Latin and local languages such as Gaulish had probably predominated. Although these older languages persisted mainly in personal and place names⁵⁸, the relatively large contribution of northern ancestry may have promoted the emergence of pre-literary Old High German as the dominant vernacular in Southern Germany and neighbouring regions.

Online content

Any methods, additional references, Nature Portfolio reporting summaries, source data, extended data, supplementary information, acknowledgements, peer review information; details of author contributions and competing interests; and statements of data and code availability are available at <https://doi.org/10.1038/s41586-026-10437-3>.

- Meier, M. *Geschichte der Völkerwanderung. Europa, Asien und Afrika vom 3. bis zum 8. Jahrhundert n. Chr.* (C. H. Beck, 2021).
- Schmidt-Hofner, S. Barbarian migrations and the economic challenges to the Roman landholding elites in the fourth century CE. *J. Late Antiq.* **10**, 372–404 (2017).
- Halsall, G. *Barbarian Migrations and the Roman West 376–568* (Cambridge Univ. Press, 2007).
- Bavuso, I. & Castrorao Barba, A. in *The European Countryside during the Migration Period: Patterns of Change from Iberia to the Caucasus (300–700 CE)* (eds Bavuso, I. & Castrorao Barba, A.) 1–11 (De Gruyter, 2023).
- Halsall, G. in *Fifth-Century Gaul: A Crisis of Identity?* (eds Drinkwater, J. & Elton, H.) 196–207 (Cambridge Univ. Press, 1992).
- Brownlee, E. Grave goods in Early Medieval Europe: regional variability and decline. *Internet Archaeol.* <https://doi.org/10.11141/ia.56.11> (2021).
- Hamerow, H. *Early Medieval Settlements: The Archaeology of Rural Communities in Northwest Europe, 400–900* (Oxford Univ. Press, 2004).
- Brather-Walter, S. in *The European Countryside during the Migration Period: Patterns of Change from Iberia to the Caucasus (300–700 CE)* (eds Bavuso, I. & Castrorao Barba, A.) 201–231 (De Gruyter, 2023).
- Theuvs, F. in *The Oxford Handbook of the Merovingian World* (eds Effros, B. & Moreira, I.) 883–915 (Oxford Univ. Press, 2020).
- Brather, S. in *Rome, Constantinople and Newly-Converted Europe. Archaeological and Historical Evidence Vol. 1* (eds Salamon, M. et al.) 333–349 (Kraków, Leipzig, Rzeszów, Warszawa, 2012).
- Sebrich, J. *Das spätantik-frühmittelalterliche Gräberfeld von Essenbach-Altheim. Materialhefte zur Bayerischen Archäologie 110* (Michael Laßleben, 2019).
- Heitmeier, I. & Haberstroh, J. *Gründerzeit: Siedlung in Bayern zwischen Spätantike und frühem Mittelalter* (EOS, 2019).
- Fehr, H. & Heitmeier, I. *Die Anfänge Bayerns. Von Raetien und Noricum zur frühmittelalterlichen Baiuvaria* (EOS, 2012).
- Veeramah, K. R. et al. Population genomic analysis of elongated skulls reveals extensive female-biased immigration in Early Medieval Bavaria. *Proc. Natl Acad. Sci. USA* **115**, 3494–3499 (2018).
- Amorim, C. E. G. et al. Understanding 6th-century barbarian social organization and migration through paleogenomics. *Nat. Commun.* **9**, 3547 (2018).
- Gretzinger, J. et al. The Anglo-Saxon migration and the formation of the early English gene pool. *Nature* **610**, 112–119 (2022).
- Patterson, N. et al. Large-scale migration into Britain during the Middle to Late Bronze Age. *Nature* **601**, 588–594 (2022).
- Antonio, M. L. et al. Stable population structure in Europe since the Iron Age, despite high mobility. *eLife* **13**, e79714 (2024).
- Vyas, D. N. et al. Fine-scale sampling uncovers the complexity of migrations in 5th–6th century Pannonia. *Curr. Biol.* **33**, 3951–3961.e11 (2023).
- Olalde, I. et al. A genetic history of the Balkans from Roman frontier to Slavic migrations. *Cell* **186**, 5472–5485.e9 (2023).
- O'Sullivan, N. et al. Ancient genome-wide analyses infer kinship structure in an Early Medieval Alemannic graveyard. *Sci. Adv.* **4**, eao1262 (2018).
- Speidel, L. et al. High-resolution genomic history of early medieval Europe. *Nature* **637**, 118–126 (2025).
- Speidel, L., Forest, M., Shi, S. & Myers, S. R. A method for genome-wide genealogy estimation for thousands of samples. *Nat. Genet.* **51**, 1321–1329 (2019).
- Lawson, D. J., Hellenthal, G., Myers, S. & Falush, D. Inference of population structure using dense haplotype data. *PLoS Genet.* **8**, e1002453 (2012).
- de Genarro, L. et al. PANE: fast and reliable ancestral reconstruction on ancient genotype data with non-negative least square and principal component analysis. *Genome Biol.* **26**, 29 (2025).
- Lee, A. D. *War in Late Antiquity: A Social History* (Blackwell, 2007).
- McColl, H. et al. Steppe ancestry in western Eurasia and the spread of the Germanic Languages. Preprint at *bioRxiv* <https://doi.org/10.1101/2024.03.13.584607> (2024).
- Velte, M. et al. Between Raetia Secunda and the duchy of Bavaria: exploring patterns of human movement and diet. *PLoS ONE* **18**, e0283243 (2023).
- Tian, Y. et al. The role of emerging elites in the formation and development of communities after the fall of the Roman Empire. *Proc. Natl Acad. Sci. USA* **121**, e2317868121 (2024).
- Treggiari, S. *Roman Marriage: Lusti Coniuges from the Time of Cicero to the Time of Ulpian* (Oxford Univ. Press, 1991).
- Frier, B. W. in *The Cambridge Ancient History: The High Empire, AD 70–192 Vol. 11* (eds Bowman, A. K., Garnsey, P. & Rathbone, D.) 787–816 (Cambridge Univ. Press, 2000).
- Barbiera, I., Castiglioni, M. & Dalla-Zuanna, G. Demography, peasantry, and family in Early Medieval Provence, 813–814. *Population* **77**, 249–274 (2022).
- Jussen, B. *Der Name der Witwe. Erkundungen zur Semantik der mittelalterlichen Bußkultur (Veröffentlichungen des Max-Planck-Instituts für Geschichte 158)* (Göttingen, 2000).
- Ubl, K. *Inzestverbot und Gesetzgebung: Die Konstruktion eines Verbrechens (300–1100)* (Millennium-Studien 20) (De Gruyter, 2008).
- Evans-Grubbs, J. in *A companion to Late Antiquity* (ed. Rousseau, P.) 201–219 (Wiley-Blackwell, 2009).
- Harper, K. in *The Oxford Handbook of Late Antiquity* (ed. Johnson, S. F.) 667–714 (Oxford, 2012).
- Wang, K. et al. Ancient DNA reveals reproductive barrier despite shared Avar-period culture. *Nature* **638**, 1007–1014 (2025).
- Saag, L. et al. North Pontic crossroads: mobility in Ukraine from the Bronze Age to the early modern period. *Sci. Adv.* **11**, ead0695 (2025).
- Gnecci-Ruscione, G. A. et al. Ancient genomes reveal origin and rapid trans-Eurasian migration of 7th century Avar elites. *Cell* **185**, 1402–1413.e21 (2022).
- Maróti, Z. et al. The genetic origin of Huns, Avars, and conquering Hungarians. *Curr. Biol.* **32**, 2858–2870.e7 (2022).
- Gretzinger, J. et al. Ancient DNA connects large-scale migration with the spread of Slavs. *Nature* **646**, 384–393 (2025).
- Akram-Lodhi, A. H. et al. (eds) *Handbook of Critical Agrarian Studies* (Edward Elgar, 2021).
- Kohl, T. *Lokale Gesellschaften: Formen der Gemeinschaft in Bayern vom 8. bis zum 10. Jahrhundert (Mittelalter-Forschungen 29)* (Ostfildern, 2010).
- Guyon, L., Guez, J., Toupance, B., Heyer, E. & Chaix, R. Patrilineal segmentary systems provide a peaceful explanation for the post-Neolithic Y-chromosome bottleneck. *Nat. Commun.* **15**, 3243 (2024).
- Guyon, L., Heyer, E., Chaix, R. Was descent in Neolithic and Bronze Age Europe patrilineal or bilateral? *Proc. Biol. Sci.* **292**, 20250815 (2025).
- Ly, G. et al. From matrimonial practices to genetic diversity in Southeast Asian populations: the signature of the matrilineal puzzle. *Philos. Trans. R.* **374**, 20180434 (2019).
- Arjava, A. *Women and Law in Late Antiquity* (Oxford Univ. Press, 1996).
- Gardner, J. F. *Women in Roman Law & Society* (Croom Helm, 1986).
- Shaw, B. D. & Saller, R. P. Close-kin marriage in Roman society? *Man* **19**, 432–444 (1984).
- Cassidy, L. M. et al. Continental influx and pervasive matrilocality in Iron Age Britain. *Nature* **637**, 1136–1142 (2025).
- Gnecci-Ruscione, G. A. et al. Network of large pedigrees reveals social practices of Avar communities. *Nature* **629**, 376–383 (2024).

52. Rivollat, M. et al. Extensive pedigrees reveal the social organization of a Neolithic community. *Nature* **620**, 600–606 (2023).
53. Brather, S. *Ethnische Interpretationen in der frühgeschichtlichen Archäologie. Geschichte, Grundlagen und Alternativen (Ergänzungsbände zum Reallexikon der germanischen Altertumskunde 42)* (Walter de Gruyter, 2004).
54. Brather, S. in *Antike im Mittelalter – Fortleben, Nachwirken, Wahrnehmung. 25 Jahre Forschungsverbund "Archäologie und Geschichte des ersten Jahrtausends in Südwestdeutschland"* (eds Brather, S. et al.) 217–234 (Ostfildern, 2014).
55. Pohl, W. in *Strategies of Identification: Ethnicity and Religion in Early Medieval Europe* (eds Pohl, W. & Heydemann, G.) 1–64 (Turnhout, 2013).
56. Schipp, O. *Der weströmische Kolonat von Konstantin bis zu den Karolingern (332 bis 861). Studien zur Geschichtsforschung des Altertums (21)* (Dr. Kovac, 2009).
57. Schulz, I. et al. Ancient genomes provide evidence of demographic shift to Slavic-associated groups in Moravia. *Genome Biol.* **26**, 259 (2025).
58. Haubrichs, W. in *The Languages of Early Medieval Charters. Latin, Germanic Vernaculars and the Written Word* (eds Gallagher, R. et al.) 68–116 (Brill, 2021).

Publisher's note Springer Nature remains neutral with regard to jurisdictional claims in published maps and institutional affiliations.



Open Access This article is licensed under a Creative Commons Attribution 4.0 International License, which permits use, sharing, adaptation, distribution and reproduction in any medium or format, as long as you give appropriate credit to the original author(s) and the source, provide a link to the Creative Commons licence, and indicate if changes were made. The images or other third party material in this article are included in the article's Creative Commons licence, unless indicated otherwise in a credit line to the material. If material is not included in the article's Creative Commons licence and your intended use is not permitted by statutory regulation or exceeds the permitted use, you will need to obtain permission directly from the copyright holder. To view a copy of this licence, visit <http://creativecommons.org/licenses/by/4.0/>.

© The Author(s) 2026

¹Palaeogenetics Group, Institute of Organismic and Molecular Evolution (iomE), Johannes Gutenberg University Mainz, Mainz, Germany. ²SNSB, Bavarian State Collection of Anthropology, Munich, Germany. ³Department of Biology, University of Fribourg, Fribourg, Switzerland. ⁴Swiss Institute of Bioinformatics, Fribourg, Switzerland. ⁵Institute of Evolutionary Biology, CSIC–Pompeu Fabra University, Barcelona, Spain. ⁶Eco-Anthropologie (UMR 7206), Muséum National d'Histoire Naturelle, CNRS, Université Paris Cité, Paris, France. ⁷Department of Genetics, Evolution and Environment, University College London, London, UK. ⁸Department of Environmental and Prevention Sciences, University of Ferrara, Ferrara, Italy. ⁹Hessian State Office for Monuments and Sites, hessenArchäologie, Marburg, Germany. ¹⁰State Office for Heritage Preservation and Archaeology Saxony-Anhalt, Halle, Germany. ¹¹Leibniz-Zentrum für Archäologie (LEIZA), Mainz, Germany. ¹²Institute of Legal Medicine, University Medical Center of the Johannes Gutenberg University Mainz, Mainz, Germany. ¹³Thüringer Landesamt für Denkmalpflege und Archäologie, Weimar, Germany. ¹⁴Royal Anthropological Institute, London, UK. ¹⁵ReVe Büro für Archäologie GbR, Bamberg, Germany. ¹⁶Stadt Villach–Museum und Archiv, Villach, Austria. ¹⁷Department of Early Historical Archaeology and Medieval Archaeology, Albert-Ludwigs-Universität Freiburg, Freiburg, Germany. ¹⁸SNSB, RiesCraterMuseum Nördlingen, Nördlingen, Germany. ¹⁹Bavarian State Office for the Conservation of Historical Monuments and Sites, Munich, Germany. ²⁰Institute of Archaeology, National Institute of the Republic of Serbia, Belgrade, Serbia. ²¹Landratsamt Deggendorf, Kreisarchäologie, Deggendorf, Germany. ²²Institut für Vor- und Frühgeschichtliche Archäologie und Provinzialrömische Archäologie, Ludwig-Maximilians-Universität München, Munich, Germany. ²³Pre- and Early Historical Archaeology, Institute of Classical Studies, Johannes Gutenberg University Mainz, Mainz, Germany. ²⁴Landratsamt Landshut, Kreisarchäologie, Essenbach, Germany. ²⁵Hessian State Office for Monuments and Sites, hessenArchäologie, Darmstadt, Germany. ²⁶Museen der Stadt Aschaffenburg, Aschaffenburg, Germany. ²⁷Institute of Ancient History, Eberhard Karls University Tübingen, Tübingen, Germany. ²⁸Institute of Medieval History, Eberhard Karls University Tübingen, Tübingen, Germany. ²⁹These authors contributed equally: Jens Blöcher, Leonardo Vallini. [✉]e-mail: steffen.patzold@uni-tuebingen.de; daniel.wegmann@unifr.ch; jburger@uni-mainz.de

Methods

Ancient DNA extraction, library preparation, sequencing, raw-read processing and variant calling followed ref. 59 (see Supplementary Information 4 and 5). Modern genomes from Deutsches Zentrum für Herz-Kreislauf-Forschung (DZHK; German Centre for Cardiovascular Research) Kiel and Munich cohorts were provided by the DZHK Heart Bank (<https://dzhk.de/dzhk-heart-bank/daten-und-bioproben/dzhkomics-ressource>). Reads were merged with ATLAS⁶⁰, duplicates were removed with sambamba⁶¹, and realigned with GATK 3.8 (ref. 62). Phasing and imputation were performed with GLIMPSE2 (refs. 63,64) using bi-allelic loci from the 1000 Genomes dataset, with a minor allele frequency >1% for shotgun genomes and autosomal 1240k SNPs⁶⁵ for array data. Mitochondrial and Y-chromosome haplotypes were assigned with haplogrep3 (ref. 66) and Yleaf2 (ref. 67).

To estimate individual birth and death dates, we developed Chronograph, a Bayesian method that integrates archaeological, radiocarbon, genetic, stratigraphic and anthropological age at death estimation (Supplementary Information 3). We used 20,000 posterior samples of birth and death dates to propagate the remaining uncertainty into downstream analyses.

Ancient genomes were projected onto a PCA of modern west Eurasian individuals taken from version 54 of the Allen Ancient DNA Resource (AARD)^{68,69} using smartpca from the EIGENSOFT package⁷⁰. Ancient individuals were taken directly from the AARD if available, or were obtained from their respective ENA repository and processed as described⁵⁹ (Supplementary Information 5). f_4 -statistics were computed using Admixtools2 (refs. 71,72).

Relate²³ and twigstats were run following the approach of ref. 22. We kept only transversion sites where no more than 5% of the genomes showed a genotype probability <0.8 when running Relate, then used twigstats to compute pairwise f_2 -statistics on inferred genealogies with a cut-off of 1,000 generations. All pairwise qpAdm models were tested, using the five European populations, plus YRI and CHB from the 1000 Genomes project⁷³ as right-populations. Individuals were clustered into sources by building a graph combining qpAdm P values and geographic information and applying Louvain clustering (see Supplementary Information 8 for details). We validated the Relate/twigstats results by re-running the same model on the same set of markers using ChromoPainter2 (ref. 24) in combination with the Bayesian ancestry inference approach implemented in sourcefindV2 (ref. 74). ChromoPainter2 was additionally run with a larger number of source individuals by adding available pre-Roman genomes sequenced on the 1240k array⁶⁵ and subsetting the dataset to only contain autosomal regions of the capture array. We used a similar clustering approach based on geography and pairwise Euclidean distances between haplotype copying vectors to identify potential source groups (see Supplementary Information 8 for details). PANE²⁵ was run using groups of individuals defined by previous publications as sources (see Supplementary Information 8 for details).

We identified runs of homozygosity using hapROH⁷⁵ on genomes with more than 400,000 SNPs on the 1240k panel⁶⁵. AnclBD was used on autosomal SNPs of the 1240k panel to detect identity-by-descent segments⁷⁶ between newly sequenced genomes and a curated set of published European individuals (Supplementary Information 10). Biological relatedness was estimated using KIN⁷⁷ and READ2 (ref. 78) with default parameters, and pedigrees reconstructed following ref. 79. Spatial coordinates for burials within graveyards were determined by overlaying the graveyard plan with a grid of arbitrary units and then recording the middle of each grave. Correlations between relatedness and burial position were assessed using Euclidean distances after grouping pairs by their degree of relatedness.

Pedigree-aware interpolation of f_4 -statistics were obtained with filia (Supplementary Information 13).

Theta was estimated using ATLAS⁶⁰, on neutral genomic regions identified in ref. 80. Deviations from Hardy-Weinberg equilibrium (F_{IS} and F_{IT}) and Hudson's F_{ST} were estimated using scikit-allele 1.3.1 (<https://github.com/cggh/scikit-allele>), on a set of bi-allelic transversions to minimize the effect of post-mortem damage.

SLiM⁸¹ simulations were used to estimate community sizes by simulating populations with monogamous mating pairs of size N [250–500] distributed across n villages [2,5], connected by migration (m – [0–1]) for 10 generations in 1,000 replicates. In each replicate S individuals were sampled (Altheim: $S = 112$, Büttelborn: $S = 40$) and relatedness (r) over three generations was calculated. A regression analysis with the Python package statsmodels (v.0.14.4)⁸² was used to determine the relationships between N , m and r for both communities, given the observed values (see Supplementary Information 16).

Strontium isotope analyses followed ref. 28 (Supplementary Information 2).

Data for maps in Fig. 1 and Supplementary Fig. 8.1 were obtained from: GEBCO Compilation Group (2022) GEBCO_2022 Grid (<https://www.gebco.net/data-products/gridded-bathymetry-data/gebco-2022>)⁸³ and Natural Earth (<https://www.naturalearthdata.com>), and plotted using R. All other maps, including Fig. 2e, Extended Data Fig. 4 and Supplementary Figs. 7.4, 8.17 and 10.1–10.7, were created using the basemap toolkit from the matplotlib library⁸⁴ in Python 3, which uses cartographic data from Generic Mapping Tools (<https://www.generic-mapping-tools.org/>).

Reporting summary

Further information on research design is available in the Nature Portfolio Reporting Summary linked to this article.

Data availability

All newly reported genome sequences have been deposited in the European Nucleotide Archive, under the accession PRJEB87112. The human reference genome (hg19) used during alignment is available via the 1000 Genomes Project⁷³ repository (https://ftp.1000genomes.ebi.ac.uk/vol1/ftp/technical/reference/phase2_reference_assembly_sequence/). Genome sequences for the 379 modern-day individuals from Germany are available upon request at the DZHK (<https://dzhk.de/en/dzhk-heart-bank/data-and-biospecimens/dzhkomics-ressource>). The 1000 Genomes Project phase 3 reference panel⁷³ used for imputation and Relate can be downloaded from <https://ftp.1000genomes.ebi.ac.uk/vol1/ftp/release/20130502/>. Previously published genotype data for present-day and ancient individuals is available through the Allen Ancient DNA Resource at the Harvard dataverse (<https://dataverse.harvard.edu/dataset.xhtml?persistentId=doi:10.7910/DVN/FFIDCW>).

Code availability

Chronograph and filia are available as git repositories at <https://bitbucket.org/wegmannlab/chronograph> and <https://bitbucket.org/wegmannlab/filia>, respectively. Additional code used in the described analyses can be found at Zenodo (<https://doi.org/10.5281/zenodo.17192653>)⁸⁵.

59. Zedda, N. et al. Biological and substitute parents in Beaker period adult-child graves. *Sci Rep.* **13**, 18765 (2023).
60. Link, V. et al. ATLAS: Analysis Tools for Low-depth and Ancient Samples. Preprint at *bioRxiv* <https://doi.org/10.1101/105346> (2017).
61. Tarasov, A., Vilella, A. J., Cuppen, E., Nijman, I. J. & Prins, P. Sambamba: fast processing of NGS alignment formats. *Bioinformatics* **31**, 2032–2034 (2015).
62. McKenna, A. et al. The Genome Analysis Toolkit: a MapReduce framework for analyzing next-generation DNA sequencing data. *Genome Res.* **20**, 1297–1303 (2010).
63. Rubinacci, S., Ribeiro, D. M., Hofmeister, R. J. & Delaneau, O. Efficient phasing and imputation of low-coverage sequencing data using large reference panels. *Nat. Genet.* **53**, 120–126 (2021).

64. Rubinacci, S., Hofmeister, R., da Mota, B. S. & Delaneau, O. Imputation of low-coverage sequencing data from 150,119 UK Biobank genomes. *bioRxiv* <https://doi.org/10.1101/2022.11.28.518213> (2022).
65. Mathieson, I. et al. Genome-wide patterns of selection in 230 ancient Eurasians. *Nature* **528**, 499–503 (2015).
66. Schönherr, S., Weissensteiner, H., Kronenberg, F. & Forer, L. Haplogrep 3—an interactive haplogroup classification and analysis platform. *Nucleic Acids Res.* **51**, W263–W268 (2023).
67. Ralf, A., González, D. M., Zhong, K. & Kayser, M. Yleaf: software for human Y-chromosomal haplogroup inference from next-generation sequencing data. *Mol. Biol. Evol.* **35**, 1291–1294 (2018).
68. Mallick, S. et al. The Allen Ancient DNA Resource (AADR) a curated compendium of ancient human genomes. *Sci. Data* **11**, 182 (2024).
69. Mallick, S. & Reich, D. The Allen Ancient DNA Resource (AADR): a curated compendium of ancient human genomes. *Harvard Dataverse* <https://doi.org/10.7910/DVN/FFIDCW> (2023).
70. Patterson, N., Price, A. L. & Reich, D. Population structure and eigenanalysis. *PLoS Genet.* **2**, e190 (2006).
71. Maier, R. et al. On the limits of fitting complex models of population history to f-statistics. *eLife* **12**, e85492 (2023).
72. Maier, R. & Patterson, N. admixtools: Inferring demographic history from genetic data. R package version 2.0.4. *GitHub* <https://github.com/uqrmaie1/admixtools> (2024).
73. 1000 Genomes Project Consortium. A global reference for human genetic variation. *Nature* **526**, 68–74 (2015).
74. Chacón-Duque, J.-C. et al. Latin Americans show wide-spread Converso ancestry and imprint of local Native ancestry on physical appearance. *Nat. Commun.* **9**, 5388 (2018).
75. Ringbauer, H., Novembre, J. & Steinrücken, M. Parental relatedness through time revealed by runs of homozygosity in ancient DNA. *Nat. Commun.* **12**, 5425 (2021).
76. Ringbauer, H. et al. Accurate detection of identity-by-descent segments in human ancient DNA. *Nat. Genet.* **56**, 143–151 (2024).
77. Popli, D., Peyrégne, S. & Peter, B. M. KIN: a method to infer relatedness from low-coverage ancient DNA. *Genome Biol.* **24**, 10 (2023).
78. Alaçamlı, E. et al. READv2: advanced and user-friendly detection of biological relatedness in archaeogenomics. *Genome Biol.* **25**, 216 (2024).
79. Blöcher, J. et al. Descent, marriage, and residence practices of a 3,800-year-old pastoral community in Central Eurasia. *Proc. Natl Acad. Sci. USA* **120**, e2303574120 (2023).
80. Pouyet, F., Aeschbacher, S., Thiéry, A. & Excoffier, L. Background selection and biased gene conversion affect more than 95% of the human genome and bias demographic inferences. *eLife* **7**, e36317 (2018).
81. Haller, B. C. & Messer, P. W. SLiM 3: forward genetic simulations beyond the Wright-Fisher model. *Mol. Biol. Evol.* **36**, 632–637 (2019).
82. Seabold, S. & Perktold, J. in *Proc. 9th Python in Science Conference* (eds van der Walt, S. & Millman, J.) 92–96 (SciPy, 2010).
83. GEBCO Compilation Group. *GEBCO 2022 Grid* <https://doi.org/10.5285/e0f0bb80-ab44-2739-e053-6c86abc0289c> (2022).
84. Hunter, J. D. Matplotlib: a 2D graphics environment. *Comput. Sci. Eng.* **9**, 90–95 (2007).
85. Wegmann, D., Eckel, R. Demography and life histories across the Roman frontier in Southern Germany 400–700 CE. *Zenodo* <https://doi.org/10.5281/zenodo.17192653> (2026).

Acknowledgements Genome data of 379 modern individuals from Germany were provided by the DZHK (FKZ: 81×1500104, 81×1500302, 81×1100101) through the DZHK Heart Bank. We thank J. Sebrich for support with the archaeological interpretation of the Altheim cemetery; S. Schade-Lindig, J. Lindenthal, the municipality of Wölfersheim, B. Herbold, J. F. Tolksdorf, G. Riedel, S. Bock, F. Immler, N. Piller, U. Schlitzer, P. Desantis, T. Trocchi and the Soprintendenza Archeologica Bologna–Modena–Reggio Emilia–Ferrara for their assistance; R. Mace and C. Papageorgopoulou for suggestions and feedback; the Viminacium excavation team; F. Siegmund; and M. Jacob, W.-R. Teegen and G. Hellenthal. Funding: Deutsche Forschungsgemeinschaft (DFG; German Research Foundation) Center for Advanced Studies 2496 ‘Migration and Mobility in Late Antiquity and the Early Middle Ages’ (M. Meier, S.P. and S.S.-H.); DFG grants BU 1403/19-1 (J. Burger) and QU 263/3-1 (D.Q.); Schweizerischer Nationalfonds (Swiss National Science Foundation) grant 310030_200420 (D.W.); European Research Council grants COREX (951385, M.G.T.), SUSTAIN (865515, M. Ivanova-Bieg), NeoMilk (324202, R. Evershed) and YMPACT (788616, V. Heyd); Wellcome Senior Research Fellowship Grant 100719/Z/12/Z (M.G.T.); DFG ‘Co-Move’ 466680522 (M.B.); DFG 555150076 (M.V.); and DFG GRK2526, project 407023052 (Y.T. and C.T.M.). We thank the University of Bern’s Next Generation Sequencing (NGS) Platform for performing the sequencing. Analyses used the MOGON2 supercomputer (<https://hpc.uni-mainz.de>) at Johannes Gutenberg University Mainz.

Author contributions Study design: J. Burger, S.P., D.W., M.H., M. Meier and S.B. Laboratory work: M.V., J.D., J. Hirsch., K. Klement, A.-L.M., M. Müller, L. Vetterditz., J.S., S.K., M.W., N.G., K. Krichel, C.T.M., F.G. and L.W. Data processing and analysis: J. Blöcher., L. Vallini., R.E., D.W., L.G., M.V., R.C., S.H., J. Burger and Y.T. Software development: D.W., R.E., P.C.-P. and A.F. Archaeological and anthropological contextualization: J. Haberstroh, S.S.-H., V.P., I.M., M.B., M.G.T., S.B., S.B.-W., J.O., S.F., T.R., R.M., D.Q., M. Marquart, C.V., D.S., G.M., B.B., N.Z., P.S., E. Seyr, K. Karpf, T.B., I.S., B.F., S.R., S.C.-W., B.P. and E. Saal. Interpretation of the results: J. Blöcher, L. Vallini., R.E., J. Burger, S.P., D.W., R.C., S.B., S.S.-H., M.H., M. Meier, T.R., R.M., M. Marquart, D.S., N.G., K. Krichel, J.S., S.K., C.T.M., F.G., L.W. and S.B.-W. Manuscript drafting: J. Burger, J. Blöcher., L. Vallini, S.P., R.E. and D.W. Revision with substantial input from: L.G., R.C., S.S.-H., J. Haberstroh, M.G.T., M.B., M.H., M. Meier, M.V. and S.B.

Funding Open access funding provided by Johannes Gutenberg-Universität Mainz.

Competing interests The authors declare no competing interests.

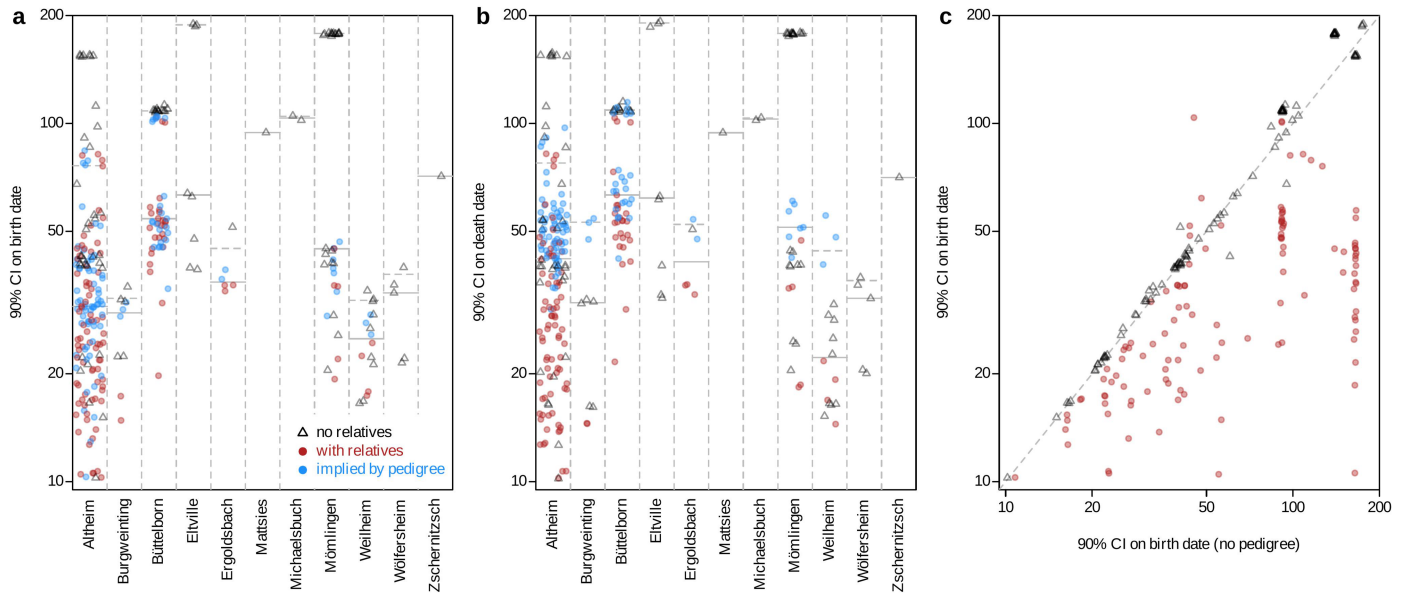
Additional information

Supplementary information The online version contains supplementary material available at <https://doi.org/10.1038/s41586-026-10437-3>.

Correspondence and requests for materials should be addressed to Steffen Patzold, Daniel Wegmann or Joachim Burger.

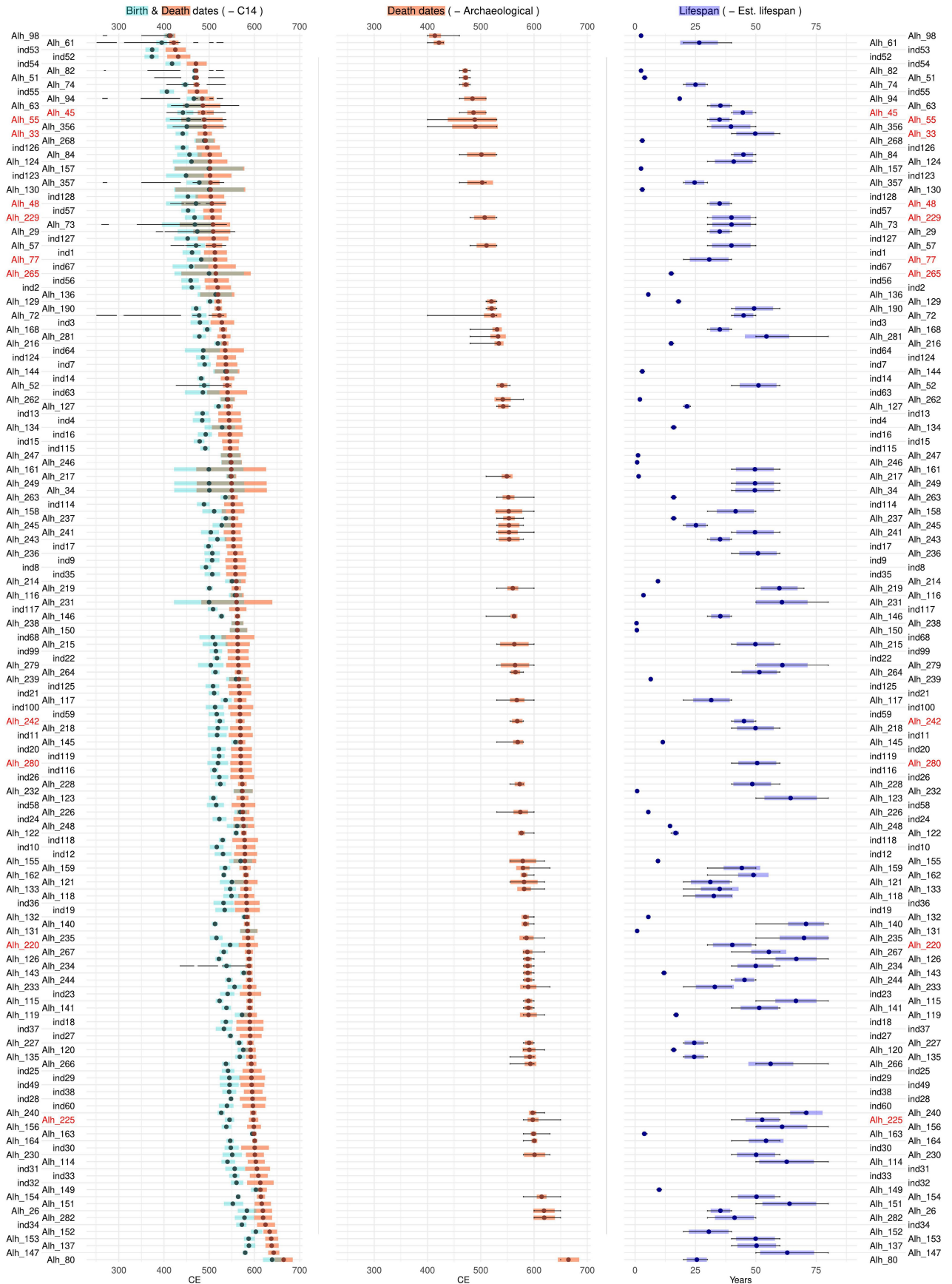
Peer review information *Nature* thanks Rebecca Flemming, Kristina Sessa, who co-reviewed with Christopher Parmenter, and the other, anonymous, reviewer(s) for their contribution to the peer review of this work.

Reprints and permissions information is available at <http://www.nature.com/reprints>.



Extended Data Fig. 1 | Estimation of Chronograph accuracy. **a** and **b**) Shown are the 90% CI on the birth (**a**) and death (**b**) dates per individual per site. Symbols and colour distinguish between sampled individuals without relatives (“no relatives”, black open triangles), sampled individuals with relatives (“with relatives”, red circles) and unsampled individuals implied by pedigree information (“implied by pedigree”, blue circles). Horizontal bars indicate the 50% and 90% quantile for each site. Credible intervals are generally much narrower for samples with relatives, i.e. for individuals whose dates are constrained by that of other individuals. This is also true for individuals that were not sampled but only implied by the pedigree, whose CI were generally

larger than for sampled individuals with relatives, but still smaller than for sampled individuals without relatives. **c**) The 90% CI on the birth date for the full run (y-axis, as in **a**) against a run that ignores pedigree information (x-axis). The strong reduction in 90% CI for most individuals with relatives illustrates the strong benefit of using pedigree information. The one outlier with strongly increased 90% CI is individual Btb73, for which pedigree information renders secondary peaks of its ^{14}C likelihood function more plausible. Note that without pedigree information, no estimation is possible on the “implied” individuals.

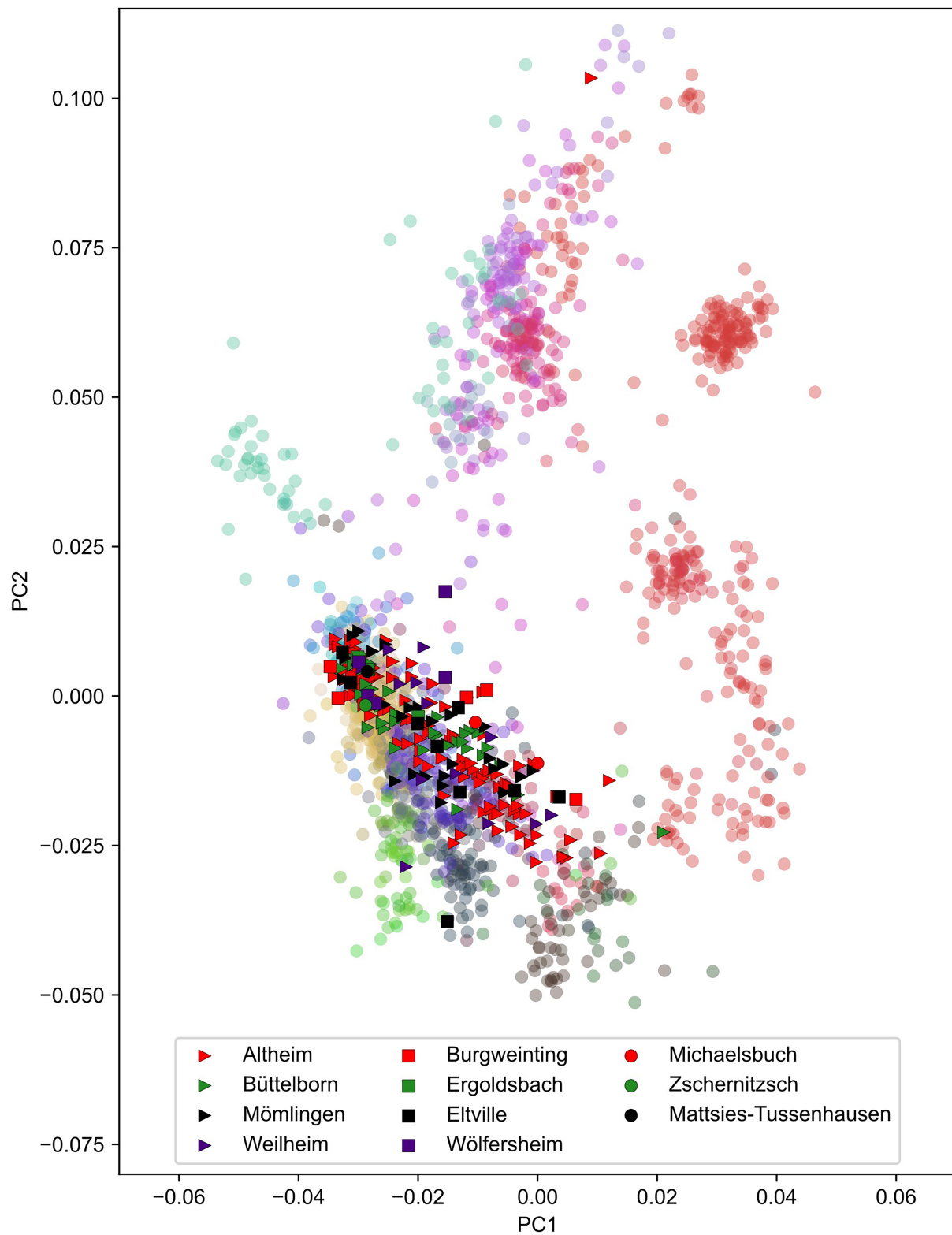


Extended Data Fig. 2 | See next page for caption.

Extended Data Fig. 2 | Life history estimates for individuals from Altheim.

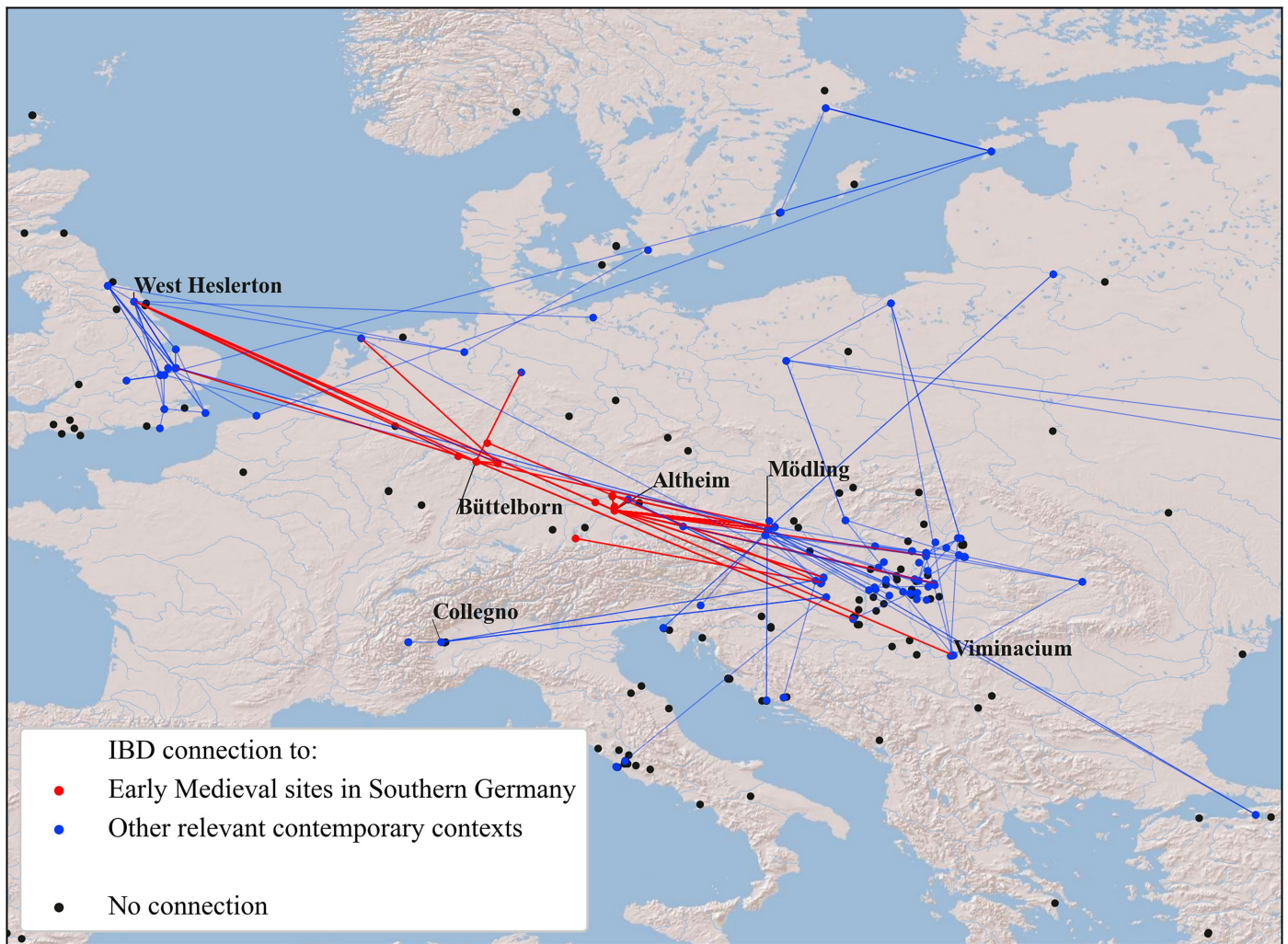
First column: posterior estimates (dot: mean, bar: 90% CI) of birth (turquoise) and death (red) dates; 90% CI of the recalibrated ^{14}C date (black line, potentially disjunct), if available. Second column: posterior estimates of death dates; 90% CI of the archaeological date of the grave (black line), if available.

Third column: posterior estimates of lifespan; 90% CI on the osteological age-at-death estimate (black line), if available. Red-coloured labels denote individuals identified as non-locals by isotopic analysis. Individuals whose names start with "ind" have not been sampled but were implied by familial relationships.



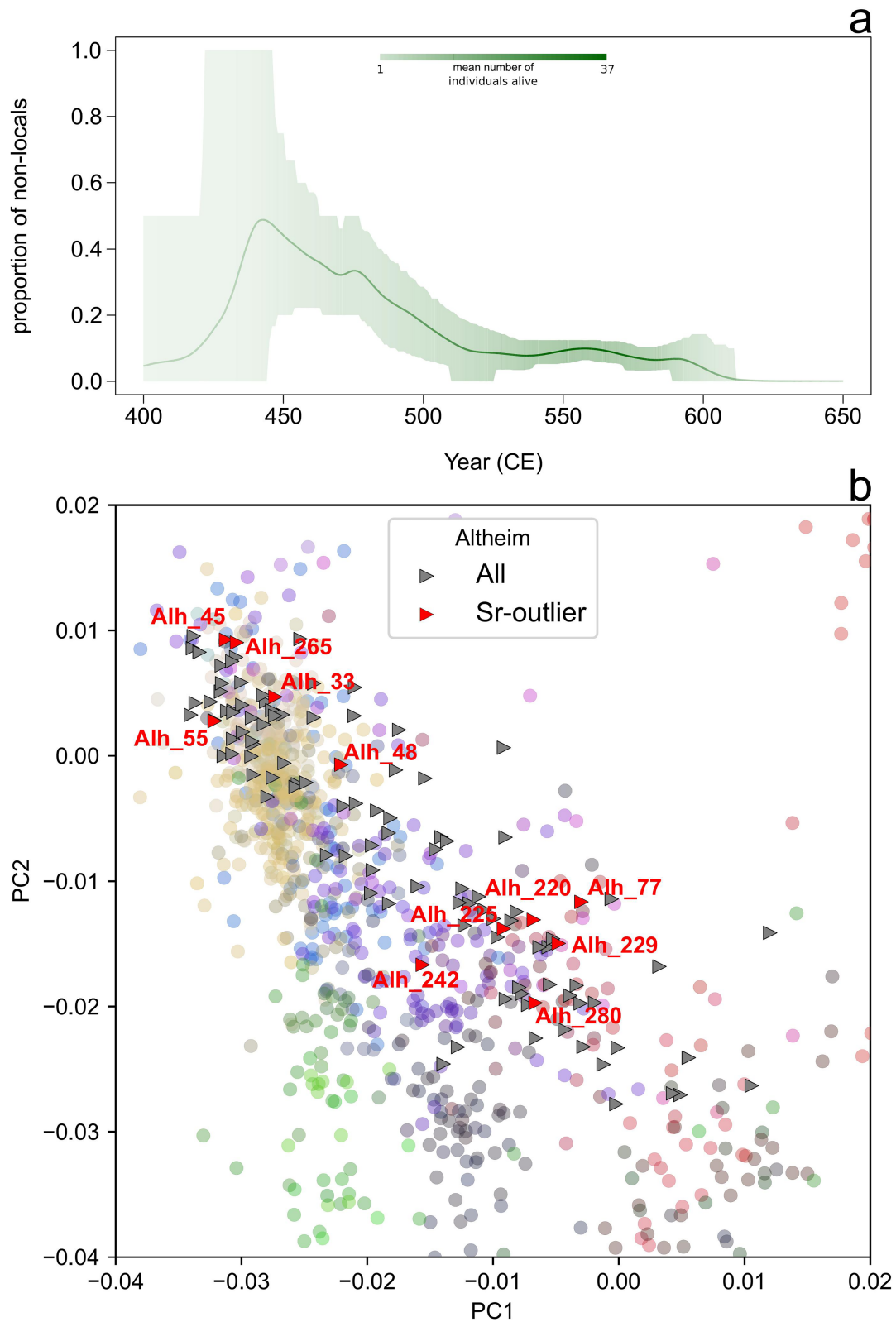
Extended Data Fig. 3 | Principal Component Analysis. First two principal components for newly sequenced Early Medieval genomes plotted alongside previously published genomes dating between 800 and 1 BCE from western Eurasia, shown as individual coloured points in the background. Colours for

the reference genomes were assigned based on the latitude/longitude coordinates listed in the AARD file and match those in Fig. 2e. Archaeological sites are symbol-coded by sample size: triangles (≥10 individuals), squares (4-9 individuals), circles (<4 individuals).



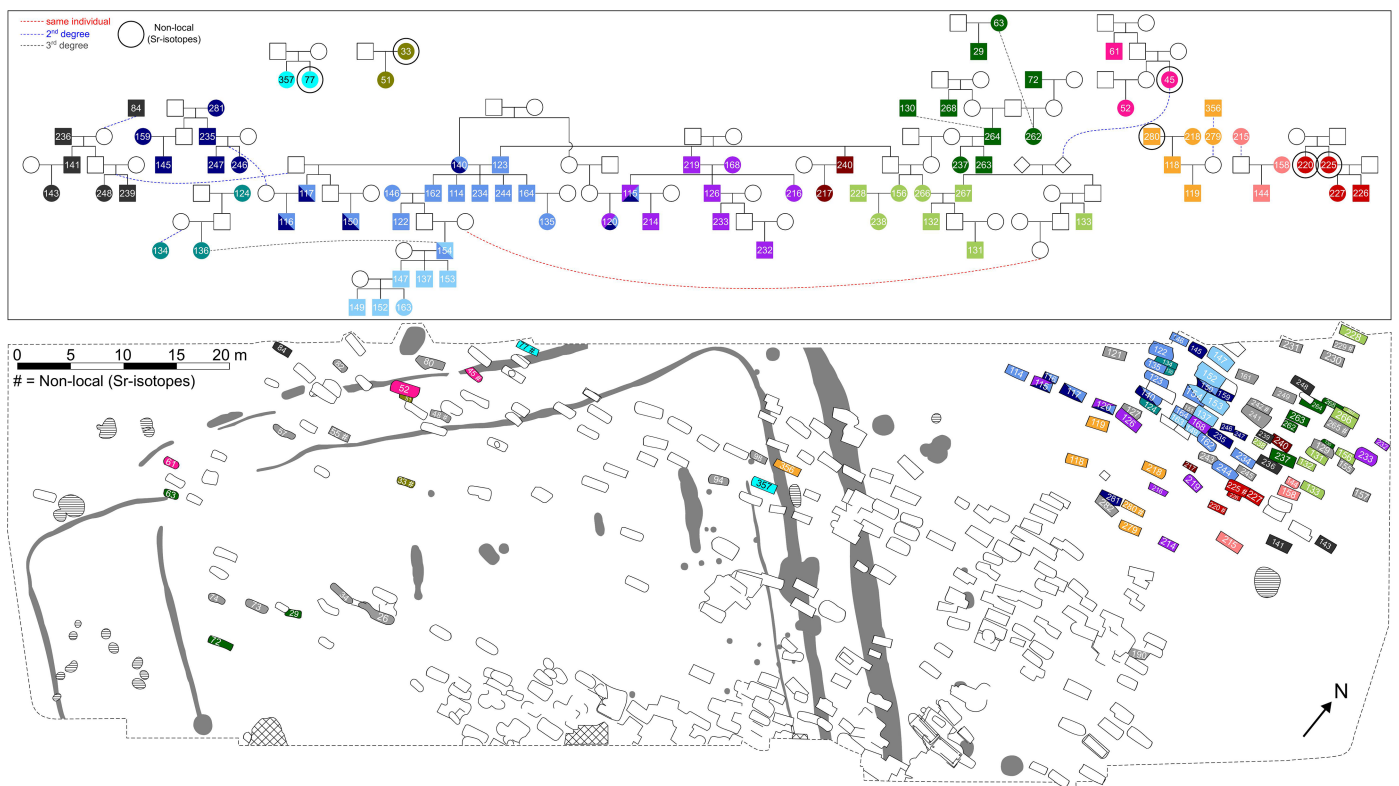
Extended Data Fig. 4 | IBD connections. Map of pairwise identical-by-descent (IBD) fragments shared between individuals from Antiquity and the Early Middle Ages (1–800 CE). Red lines connect newly published Late-Antique and Early-Medieval individuals from southern Germany who share at least one ≥ 20 cM genomic segment; light-blue lines indicate analogous links among

previously published contemporaneous genomes. The overwhelming majority of IBD tracts occur between individuals with a northern-European ancestry profile. Sites with the highest number of sampled individuals in each region are labelled by name.



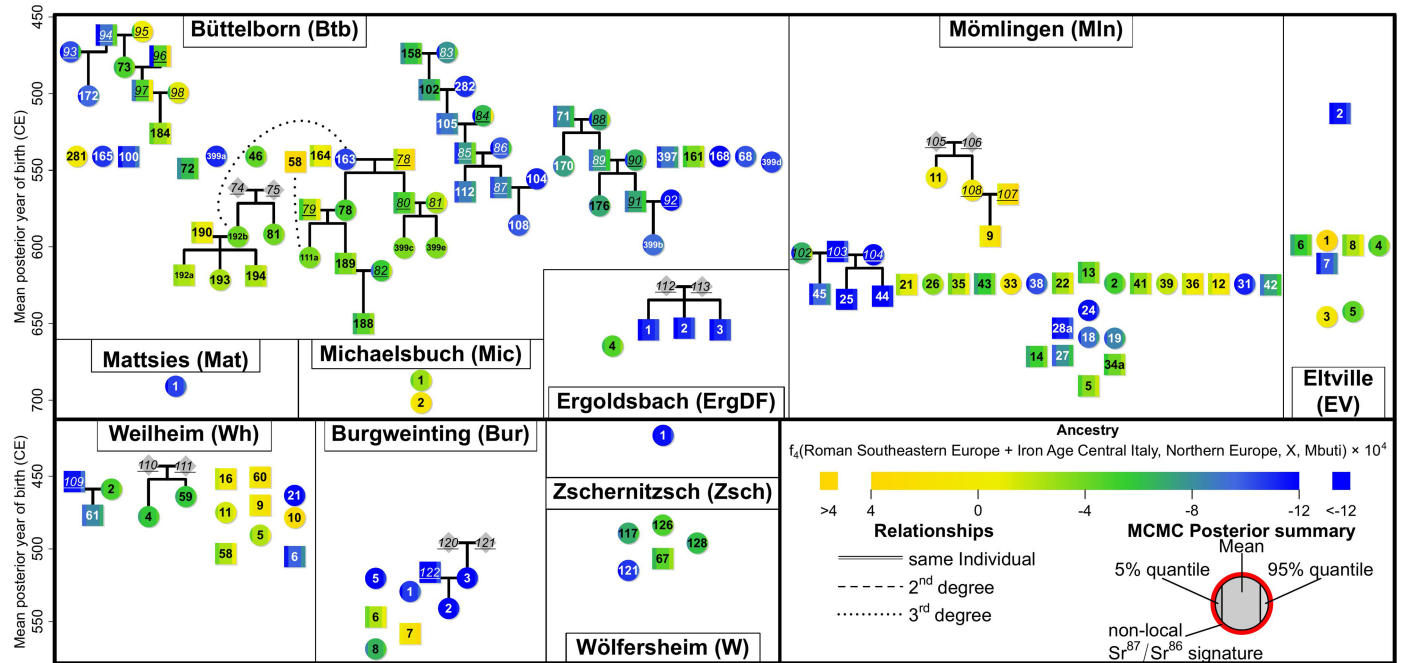
Extended Data Fig. 5 | Non-local individuals. **a.** Fraction of non-local individuals in the Altheim population, inferred from $^{87}\text{Sr}/^{86}\text{Sr}$ ratios. Values were computed annually across 15000 MCMC iterations generated by Chronograph; the solid line shows the mean, and the shaded area represents the 90% credible interval (5th–95th percentiles). Plot transparency reflects the

mean number of individuals alive at each time point across all iterations. **b.** Principal component analysis (PCA) of Altheim individuals (grey triangles), with those exhibiting non-local strontium isotope signatures highlighted in red.



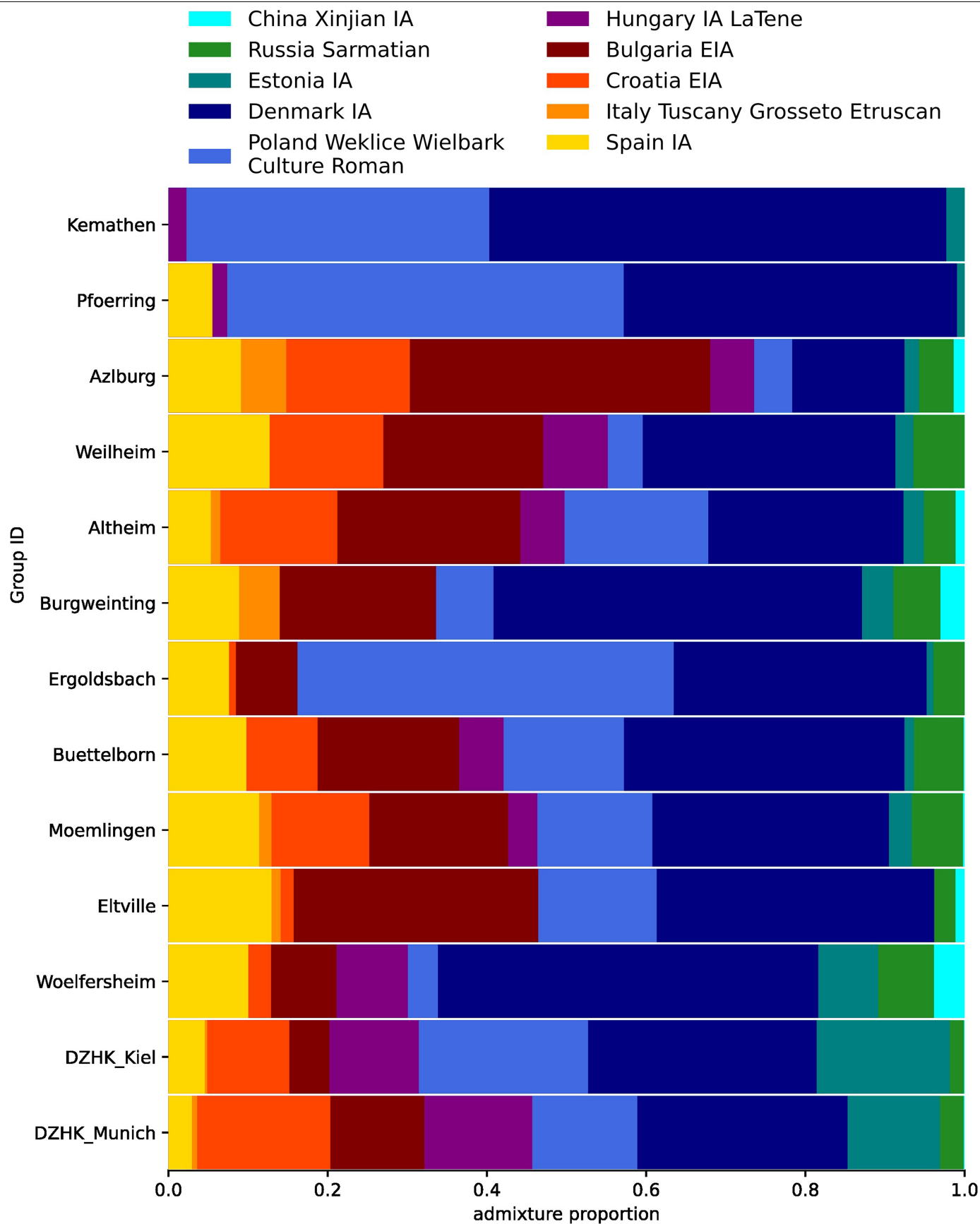
Extended Data Fig. 6 | Spatial distribution of family lineages in the Altheim graveyard. Grave plan courtesy of Bayerisches Landesamt für Denkmalpflege; Dr. Johannes Sebrich.

Article



Extended Data Fig. 7 | Reconstructed pedigrees from sites other than Altheim. Pedigrees are color-coded according to f_4 -statistic results and displayed in chronological order. Sequenced individuals are shown in bold,

individuals inferred from pedigree structures, are shown in italics and underlined. Individuals not connected to any pedigree are included for contextual reference.



Extended Data Fig. 8 | Ancestry estimates from PANE using a 10-population model. Bars represent average ancestry proportions for genomes from archaeological sites from Germany (sequenced in this study) spanning Late

Antiquity to the Early Medieval period, as well as for the two DZHK reference cohorts from Munich and Kiel.

Article

Extended Data Table 1 | Population genetic statistics

	Altheim	Büttelborn	Mömlingen	Weilheim	Kiel	Munich
number of individuals	112	40	28	13	194	185
% of individuals with a 1st-3rd degree relative	66.6 - 83.4	55.8 - 84.2	5.9 - 36.1	5.9 - 56.1	0	0
Est. % of adults sampled	38.1 (21.7 - 55.0)	41.1 (15.5 - 7.9)	/	/	/	/
Est. community size per generation and settlement (5 village model)	41-70	23-54	/	/	/	/
Mean of pairwise shared IBD fragments >8 centimorgan - both sexes	87.59 ± 4.66	114.87 ± 17.44	26.48 ± 9.31	87.27 ± 47.95	0.05 ± 0.01	0.27 ± 0.20
pairs with 0 IBDs >8cM [%]	77.5	87.58	92.59	91.03	99.52	98.17
Mean pairwise shared IBD fragments >8 centimorgan - all females	30.92 ± 5.28	98.52 ± 27.49	12.62 ± 8.70	131.16 ± 100.65	0.03 ± 0.01	0.35 ± 0.5
Mean pairwise shared IBD fragments >8 centimorgan - all males	170.55 ± 13.08	183.15 ± 54.99	40.96 ± 20.29	0.00 ± 0.00	0.05 ± 0.01	0.23 ± 0.03
mt haplotype diversity (CI)	0.99 (0.93 - 1.04)	0.99 (0.89 - 1.08)	0.98 (0.91 - 1.04)	0.97 (0.79 - 1.15)	0.89 (0.86-0.92)	0.94 (0.92-0.95)
Y haplotype diversity (CI)	0.86 (0.51 - 1.20)	1.00 (0.55 - 1.45)	0.65 (0.34 - 0.96)	0.50 (-0.15 - 1.15)	0.62 (0.51-0.73)	0.65 (0.54-0.76)
Genome wide $\theta + CI * 10^3$	1.27 (0.91 - 2.61)	1.13 (0.85 - 2.16)	1.13 (1.00 - 1.28)	1.18 (0.97 - 1.29)	1.59 (1.55-1.62)	1.59 (1.55-1.63)
$F_{is} + 95\% CI$	0.22 (0.21-0.24)	0.20 (0.18-0.22)	0.19 (0.17-0.21)	0.07 (0.04-0.09)	-0.0050 (-0.0108-0.0008)	-0.0054 (-0.0110-0.0001)
$F_{st} + 95\% CI$ between	Altheim - Büttelborn	Altheim - Mömlingen	Büttelborn - Mömlingen	Weilheim - Altheim	Weilheim-Büttelborn	Weilheim-Mömlingen
	0.0103 (0.0065-0.0144)	0.0046 (0.0025-0.0070)	0.0106 (0.0061-0.0151)	0.0063 (0.0029-0.0096)	0.0106 (0.0053-0.0165)	0.0067 (0.0029-0.0107)
	Kiel - Munich					
	0.0002 (0.0000-0.0005)					
$F_{it} + 95\% CI$	Early Medieval sites Southern Germany				Modern Munich + Kiel	
	0.23 (0.22-0.24)				-0.0035 (-0.0081-0.0009)	

Calculated from unrelated individuals at the four main Early Medieval sites and from modern DZHK genomes from Kiel and Munich, Germany. Only transversions were used for estimates on autosomal markers, except for theta (θ), which was estimated on a set of "neutral" regions defined in⁸⁰.

Reporting Summary

Nature Portfolio wishes to improve the reproducibility of the work that we publish. This form provides structure for consistency and transparency in reporting. For further information on Nature Portfolio policies, see our [Editorial Policies](#) and the [Editorial Policy Checklist](#).

Statistics

For all statistical analyses, confirm that the following items are present in the figure legend, table legend, main text, or Methods section.

n/a Confirmed

- The exact sample size (n) for each experimental group/condition, given as a discrete number and unit of measurement
- A statement on whether measurements were taken from distinct samples or whether the same sample was measured repeatedly
- The statistical test(s) used AND whether they are one- or two-sided
Only common tests should be described solely by name; describe more complex techniques in the Methods section.
- A description of all covariates tested
- A description of any assumptions or corrections, such as tests of normality and adjustment for multiple comparisons
- A full description of the statistical parameters including central tendency (e.g. means) or other basic estimates (e.g. regression coefficient) AND variation (e.g. standard deviation) or associated estimates of uncertainty (e.g. confidence intervals)
- For null hypothesis testing, the test statistic (e.g. F , t , r) with confidence intervals, effect sizes, degrees of freedom and P value noted
Give P values as exact values whenever suitable.
- For Bayesian analysis, information on the choice of priors and Markov chain Monte Carlo settings
- For hierarchical and complex designs, identification of the appropriate level for tests and full reporting of outcomes
- Estimates of effect sizes (e.g. Cohen's d , Pearson's r), indicating how they were calculated

Our web collection on [statistics for biologists](#) contains articles on many of the points above.

Software and code

Policy information about [availability of computer code](#)

Data collection Newly reported data was generated on the Illumina NovaSeq 6000 and co-analysed alongside publicly available sequence data.

Data analysis

```
trimmomatic 0.36
bwa 0.7.17-r1188
SAMtools 1.13
sambamba 0.6.8
GATK 3.8
contamMix 1.0.9
ATLAS commit [647daf792df01c4aa8e686de0e462ddd8f91e6c6]
glimpse2
HaploGrep3
Yleaf2
BCFtools 1.13
plink 1.9
EIGENSOFT (smartpca) v8.0.0
ADMIXTOOLS 2.0.8
filia commit [2fa4117fc22597a106769e8d12758f7c33c51f75]
Chronograph commit
[affa83ffb04c6083d6fdf71a506b09ac0300fe74]
scikit-allele v1.3.1
statsmodels v.0.14.4
```

SLiM 4
 pixy 1.2.7
 hapROH 0.64
 anclBD 0.5
 twigstats 1.0.2
 Relate 1.2.2
 finestructure4
 ChromoPainter2
 SourceFind2
 PANE 0.0.1
 Additional code used in the analyses: <https://doi.org/10.5281/zenodo.17192653>

For manuscripts utilizing custom algorithms or software that are central to the research but not yet described in published literature, software must be made available to editors and reviewers. We strongly encourage code deposition in a community repository (e.g. GitHub). See the Nature Portfolio [guidelines for submitting code & software](#) for further information.

Data

Policy information about [availability of data](#)

All manuscripts must include a [data availability statement](#). This statement should provide the following information, where applicable:

- Accession codes, unique identifiers, or web links for publicly available datasets
- A description of any restrictions on data availability
- For clinical datasets or third party data, please ensure that the statement adheres to our [policy](#)

Raw and aligned sequence reads are available at the European Nucleotide Archive under accession number PRJEB87112. The human reference genome (hg19) used during alignment is available via the 1000 genomes project repository (https://ftp.1000genomes.ebi.ac.uk/vol1/ftp/technical/reference/phase2_reference_assembly_sequence/). Genome sequences for the 379 modern day individuals from Germany are available upon request at the DZHK (<https://dzhk.de/en/dzhk-heart-bank/data-and-biospecimens/dzhkomics-resource>). The 1000GP phase 3 reference panel used for imputation and Relate can be downloaded from <https://ftp.1000genomes.ebi.ac.uk/vol1/ftp/release/20130502/>. Previously published genotype data for present-day and ancient individuals is available through the Allen Ancient DNA Resource at the Harvard dataverse (<https://dataverse.harvard.edu/dataset.xhtml?persistentId=doi:10.7910/DVN/FFIDCW>).

Research involving human participants, their data, or biological material

Policy information about studies with [human participants or human data](#). See also policy information about [sex, gender \(identity/presentation\), and sexual orientation](#) and [race, ethnicity and racism](#).

Reporting on sex and gender	Assignments of male/female were based on the distribution of reads aligned to the sex chromosomes. Genomes were grouped based on these assignments to draw conclusions about residence, marriage and kinship practices.
Reporting on race, ethnicity, or other socially relevant groupings	We did not categorize individuals by socially constructed categories such as ethnicity or race. Samples were grouped by geography, dating as well as funerary context. We furthermore used genomic ancestry and affinities to other geographic and temporally defined groups of individuals to assess demographic processes at local scales.
Population characteristics	Osteological assessments of age-at-death, pathologies and potential trauma was carried out for some of the individuals in this study. We determined individual ancestry, shared genomic segments and affinities to other spatiotemporally defined groups.
Recruitment	NA
Ethics oversight	NA

Note that full information on the approval of the study protocol must also be provided in the manuscript.

Field-specific reporting

Please select the one below that is the best fit for your research. If you are not sure, read the appropriate sections before making your selection.

Life sciences Behavioural & social sciences Ecological, evolutionary & environmental sciences

For a reference copy of the document with all sections, see nature.com/documents/nr-reporting-summary-flat.pdf

Life sciences study design

All studies must disclose on these points even when the disclosure is negative.

Sample size	NA
Data exclusions	NA
Replication	NA

Randomization

NA

Blinding

NA

Behavioural & social sciences study design

All studies must disclose on these points even when the disclosure is negative.

Study description

NA

Research sample

NA

Sampling strategy

NA

Data collection

NA

Timing

NA

Data exclusions

NA

Non-participation

NA

Randomization

NA

Ecological, evolutionary & environmental sciences study design

All studies must disclose on these points even when the disclosure is negative.

Study description

We generated 258 genomes with a main focus on early medieval row-gravefields from southern Germany, with the intend to characterize the populations that started these customs and their social and kinship practices. Additionally we generated data from key sites dating to late Antiquity and the Iron Age for contextualization.

Research sample

Sequence data generated from human remains from different archaeological contexts

Sampling strategy

For the four main sites we intended to generate a sample large enough to be able to capture temporal trends and identify potential kinship systems. Additional individuals from archaeological sites in the same regions were chosen for contextualization.

Data collection

The majority of newly reported data (239) was generated from individuals found during archaeological excavations in southern Germany, with additional data from individuals from northern Italy (2), Austria (3), Romania (3) Serbia (10) and Turkey(1). Bone samples were collected and transferred to the clean-room facilities of the Palaeogenetics Group of the JGU Mainz for further processing.

Timing and spatial scale

NA

Data exclusions

We created a subset of the data that excluded close-kin pairs for population genetic analyses. Data was excluded from certain analyses based on ancestry, geographical or temporal range. Specific data used and rationale for exclusion are given in the respective sections of the manuscript and the Supplementary Information.

Reproducibility

All data will be published alongside this study to ensure reproducibility

Randomization

NA

Blinding

NA

Did the study involve field work?

 Yes

 No

Field work, collection and transport

Field conditions

NA

Location

NA

Access & import/export

NA

Disturbance

NA

Reporting for specific materials, systems and methods

We require information from authors about some types of materials, experimental systems and methods used in many studies. Here, indicate whether each material, system or method listed is relevant to your study. If you are not sure if a list item applies to your research, read the appropriate section before selecting a response.

Materials & experimental systems

Methods

- n/a Involved in the study
- Antibodies
- Eukaryotic cell lines
- Palaeontology and archaeology
- Animals and other organisms
- Clinical data
- Dual use research of concern
- Plants

- n/a Involved in the study
- ChIP-seq
- Flow cytometry
- MRI-based neuroimaging

Antibodies

Antibodies used

NA

Validation

NA

Eukaryotic cell lines

Policy information about [cell lines and Sex and Gender in Research](#)

Cell line source(s)

NA

Authentication

NA

Mycoplasma contamination

NA

Commonly misidentified lines
(See [ICLAC](#) register)

NA

Palaeontology and Archaeology

Specimen provenance

All samples were provided by co-authors/collaborators of this study who held the necessary permissions to sample those specimen for the analyses reported here.

Specimen deposition

Bone residuals from DNA sampling are stored in the clean room facilities of the Palaeogenetics Group, JGU Mainz

Dating methods

New radiocarbon dates were generated at the Curt-Engelhorn-Center for Archaeometry, Mannheim, Germany, the AMS laboratory Erlangen, Friedrich-Alexander Universität Erlangen-Nürnberg, Germany and Mass Spectrometry Laboratory, Center for Physical Sciences and Technology, in Vilnius, Lithuania. Laboratory protocols and further details can be found at each laboratories website.

Tick this box to confirm that the raw and calibrated dates are available in the paper or in Supplementary Information.

Ethics oversight

All genomes published alongside this study originate from archaeological contexts and have no identifiable relationships to living persons.

Note that full information on the approval of the study protocol must also be provided in the manuscript.

Animals and other research organisms

Policy information about [studies involving animals](#); [ARRIVE guidelines](#) recommended for reporting animal research, and [Sex and Gender in Research](#)

Laboratory animals

NA

Wild animals

NA

Reporting on sex	NA
Field-collected samples	NA
Ethics oversight	NA

Note that full information on the approval of the study protocol must also be provided in the manuscript.

Clinical data

Policy information about [clinical studies](#)

All manuscripts should comply with the ICMJE [guidelines for publication of clinical research](#) and a completed [CONSORT checklist](#) must be included with all submissions.

Clinical trial registration	NA
Study protocol	NA
Data collection	NA
Outcomes	NA

Dual use research of concern

Policy information about [dual use research of concern](#)

Hazards

Could the accidental, deliberate or reckless misuse of agents or technologies generated in the work, or the application of information presented in the manuscript, pose a threat to:

No	Yes	
<input checked="" type="checkbox"/>	<input type="checkbox"/>	Public health
<input checked="" type="checkbox"/>	<input type="checkbox"/>	National security
<input checked="" type="checkbox"/>	<input type="checkbox"/>	Crops and/or livestock
<input checked="" type="checkbox"/>	<input type="checkbox"/>	Ecosystems
<input checked="" type="checkbox"/>	<input type="checkbox"/>	Any other significant area

Experiments of concern

Does the work involve any of these experiments of concern:

No	Yes	
<input checked="" type="checkbox"/>	<input type="checkbox"/>	Demonstrate how to render a vaccine ineffective
<input checked="" type="checkbox"/>	<input type="checkbox"/>	Confer resistance to therapeutically useful antibiotics or antiviral agents
<input checked="" type="checkbox"/>	<input type="checkbox"/>	Enhance the virulence of a pathogen or render a nonpathogen virulent
<input checked="" type="checkbox"/>	<input type="checkbox"/>	Increase transmissibility of a pathogen
<input checked="" type="checkbox"/>	<input type="checkbox"/>	Alter the host range of a pathogen
<input checked="" type="checkbox"/>	<input type="checkbox"/>	Enable evasion of diagnostic/detection modalities
<input checked="" type="checkbox"/>	<input type="checkbox"/>	Enable the weaponization of a biological agent or toxin
<input checked="" type="checkbox"/>	<input type="checkbox"/>	Any other potentially harmful combination of experiments and agents

Plants

Seed stocks	NA
Novel plant genotypes	NA
Authentication	NA

ChIP-seq

Data deposition

- Confirm that both raw and final processed data have been deposited in a public database such as [GEO](#).
- Confirm that you have deposited or provided access to graph files (e.g. BED files) for the called peaks.

Data access links <i>May remain private before publication.</i>	NA
Files in database submission	NA
Genome browser session (e.g. UCSC)	NA

Methodology

Replicates	NA
Sequencing depth	NA
Antibodies	NA
Peak calling parameters	NA
Data quality	NA
Software	NA

Flow Cytometry

Plots

Confirm that:

- The axis labels state the marker and fluorochrome used (e.g. CD4-FITC).
- The axis scales are clearly visible. Include numbers along axes only for bottom left plot of group (a 'group' is an analysis of identical markers).
- All plots are contour plots with outliers or pseudocolor plots.
- A numerical value for number of cells or percentage (with statistics) is provided.

Methodology

Sample preparation	NA
Instrument	NA
Software	NA
Cell population abundance	NA

Gating strategy

NA

Tick this box to confirm that a figure exemplifying the gating strategy is provided in the Supplementary Information.

Magnetic resonance imaging

Experimental design

Design type

NA

Design specifications

NA

Behavioral performance measures

NA

Acquisition

Imaging type(s)

NA

Field strength

NA

Sequence & imaging parameters

NA

Area of acquisition

NA

Diffusion MRI

 Used Not used

Preprocessing

Preprocessing software

NA

Normalization

NA

Normalization template

NA

Noise and artifact removal

NA

Volume censoring

NA

Statistical modeling & inference

Model type and settings

NA

Effect(s) tested

NA

Specify type of analysis: Whole brain ROI-based Both

Statistic type for inference

NA

(See [Eklund et al. 2016](#))

Correction

NA

Models & analysis

n/a | Involved in the study

 Functional and/or effective connectivity Graph analysis Multivariate modeling or predictive analysis

Functional and/or effective connectivity

NA

Graph analysis

NA

Multivariate modeling and predictive analysis

NA